# Pentagram Rigidity for Centrally Symmetric Octagons

Richard Evan Schwartz [*]

January 11, 2024

## Abstract

In this paper I will establish a special case of a conjecture that intertwines the deep diagonal pentagram maps and Poncelet polygons. The special case is that of the 3-diagonal map acting on affine equivalence classes of centrally symmetric octagons. The proof involves establishing that the map is Arnold-Liouville integrable in this case, and then exploring the Lagrangian surface foliation in detail.

## 1 Introduction

Given an $n$-gon $P_0$, we let $P_1 = T_k(P_0)$ be the $n$-gon obtained by intersecting the successive $k$-diagonals of $P_0$. For $k = 2$ the map $T_k$ is known as the *pentagram map* and it is a well-studied dynamical system. When $k > 2$ the map is often called a *deep diagonal map*. Figure 1 below shows two examples of the 3-diagonal map $T_3$ acting on 8-gons. The map $T_k$ is generically defined and invertible. The deep diagonal maps are amongst the simplest of many generalizations of the pentagam map. See e.g. [3], [4], [5], [7], [8], [9], [11], [12], [13], [14], [15], [18], [19], [20], [25], [26] for results about the pentagram map and its generalizations.

The diagonal maps interact nicely with Poncelet polygons. A *Poncelet polygon* in the projective plane is a polygon which is inscribed in one conic section and circumscribed about another. Poncelet polygons are classic objects in projective geometry. In [20] I proved that if $P$ is a Poncelet $n$-gon

**Address:** Department of Mathematics, Brown University, 151 Thayer Street, Providence, RI, 02912, USA
**Email:** Richard.Evan.Schwartz@gmail.com

and $n$ is odd then $T_k(P)$ and $P$ are projectively equivalent. I gave the proof in the odd case just for convenience; I am sure that the result holds in the even case as well.

A polygon in the projective plane is *convex* if it is projectively equivalent to a planar convex polygon. In [7], a much more recent and advanced work, A. Izosimov proves that if $P$ is a convex polygon and $T_2(P)$ is projectively equivalent to $P$, then $P$ is a Poncelet polygon. This result can fail e.g. for certain non-convex polygons in the complex projective plane.
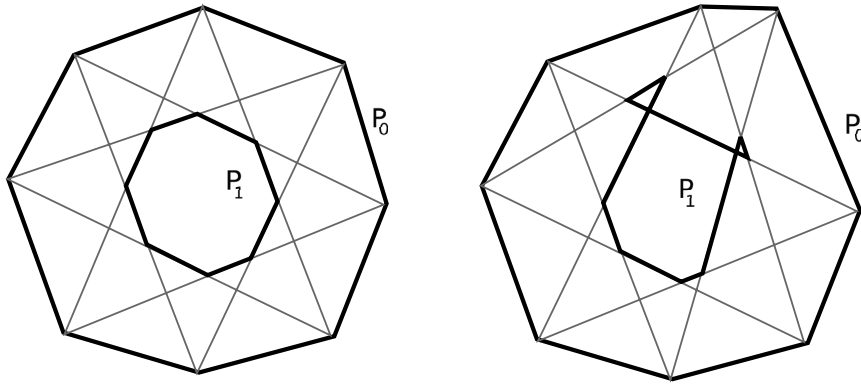


Figure 1: $P_0$ and $P_1 = T_3(P_0)$.

The maps $T_k$ and $T_k^{-1}$ are always defined on convex $n$-gons. As Figure 1 shows, the map $T_3$ need not preserve convexity. Starting with $P_0$ we define the *k-diagonal orbit* to be the bi-infinite sequence $\{P_j\}$ where $P_j = T_k^j(P_0)$. My result about Poncelet polygons implies that if $P_0$ is convex and Poncelet then $P_j$ is convex (and Poncelet) for all $j \in \mathbf{Z}$. Here is a deeper conjecture about how the deep diagonal maps interact with Poncelet polygons – no pun intended.

**Conjecture 1.1 (Pentagram Rigidity)** *Let $(n, k)$ be relatively prime with $n \geq 7$ and $3 \leq k < n/2$. Let $P_0$ be a convex $n$-gon and let $\{P_j\}$ be its $k$-diagonal orbit. Then $P_0$ is a convex Poncelet polygon if and only if $\{P_j\}$ is convex for all $j \in \mathbf{Z}$.*

I have been talking, occasionally and informally, about this conjecture for about 35 years but I only recently formally wrote it down in [21]. Originally I concieved of the Pentagram Rigidity conjecture as a projective geometry analogue of circle-packing rigidity. The first such circle packing rigidity paper is [16]. See [17] for a much broader and more definitive work on circle packing rigidity.

Let me comment on the constraints on $k$ and $n$. When $k = 2$ the conjecture fails because $T_2$ preserves convexity. I did enough experimenting to convince myself (without a formal proof) that when $k$ and $n$ are even, the map $T_k^2$ is the identity mod scale on semi-regular $n$-gons. These are polygons with $n$-fold but not necessarily $2n$-fold dihedral symmetry. In any case, one can pick a concrete example to furnish a counter-example to the conjecture when $k$ and $n$ are both even. Perhaps the conjecture holds in the more general situation that $k$ and $n$ are not both even, but I would prefer to make a more cautious conjecture.

In [22] I proved Conjecture 1.1 for the case of 8-gons with 4-fold rotational symmetry. In this toy case, the relevant moduli space is 2-dimensional and foliated by $T_3$-invariant elliptic curves. The other "simplest case", that of 7-gons with bilateral symmetry, is similar.

In this paper I will prove the first really nontrivial case of the conjecture. An even-sided polygon $P$ is *centrally symmetric* if it is invariant with respect to the map $p \to -p$.

**Theorem 1.2 (Main)** *The Pentagram Rigidity Conjecture is true for $(8,3)$ provided that the octagon is centrally symmetric.*

This case is attractive for two reasons. First, the analysis goes beyond elliptic curves. Second, this is the first case in which the full Poncelet families arise. Very few Poncelet 8-gons have 4-fold symmetry, but all Poncelet 8-gons (and indeed all even-sided Poncelet polygons) are centrally symmetric. See [6].

Our proof will show the stronger result that the forward orbit remains convex if and only if $P_0$ is inscribed in an ellipse. It is already a theorem in [2] that if an octagon (not necessarily centrally symmetric) is inscribed in an ellipse then so its image under $T_3$. See also [23]. In §7, when I treat the case of inscribed and circumscribed 8-gons, I will obtain the following additional result about the inscribed case.

**Theorem 1.3** *Let $P_0$ be a convex centrally symmetric 8-gon which is not Poncelet but which is still inscribed in an ellipse. Then $P_k$ converges to a convex Poncelet 8-gon as $k \to -\infty$ and (if the iterates are all defined) to a star-convex Poncelet 8-gon as $k \to +\infty$. Up to affine transformation, the two limits have the same vertex set and the vertex orders are related by the star-reordering:* $12345678 \to 14725836$.

The Main Theorem derives from a structural result about $T_3$. Let $\mathcal{P}_{8,2}$ denote the space of affine equivalence classes of centrally symmetric 8-gons. We choose coordinates so that $\mathcal{P}_{8,2}$ is an open dense subset of $\boldsymbol{R}^4$.

**Theorem 1.4 (Integrability)** *The action of $T_3$ on the 4-dimensional space $\mathcal{P}_{8,2}$ has an invariant (singular) symplectic form and 2 algebraically independent rational invariants which Poisson commute with respect to it.*

I found the invariant symplectic form and the algebraic invariants by guesswork, and then their verification is quite straightforward. At the end of §2.3 I will give more motivation and relate the invariants somewhat to the literature. Integrability is a main theme in the study of $T_2$, and indeed the pentagram map is one of the best known discrete completely integrable system. Certain integrability results are known for $T_k$ for all $k \geq 2$. It is proved in [5] that $T_k$ is completely integrable when defined on the space of so-called *twisted, corrugated* polygons. A general integrability result, Theorem 6.2 in [9], covers the action of $T_3$ on the space of projective classes of ordinary polygons, but it seems difficult to extract from [5] and [9] an explicit integrability result like Theorem 1.4. Interestingly, one also sees integrable systems arise in circle packings. There are a number of works about this; see e.g. [1].
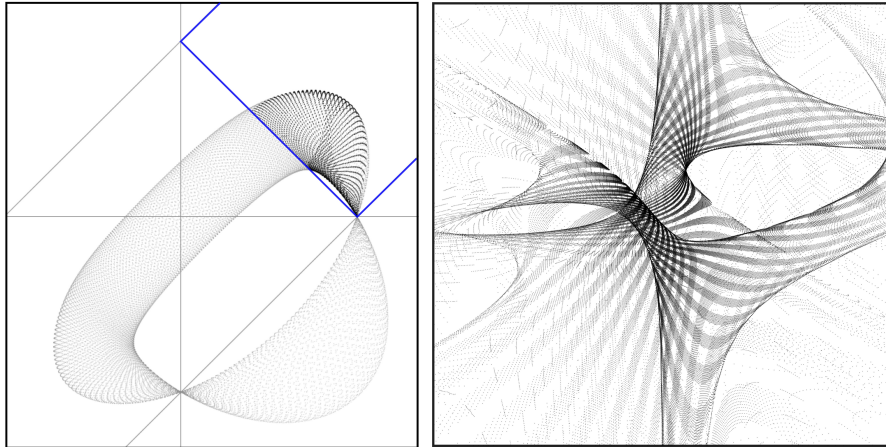


Figure 2: A torus orbit and a beautiful orbit.

Figure 2 (left) illustrates how Theorem 1.4 helps prove the Main Theorem. This picture shows a planar projection of the first $2^{15}$ points of an orbit that starts with a point representing a convex 8-gon. The metric completion of the orbit is a torus. The darkly shaded part of the orbit is (as we prove) a cylinder $L_+$ which properly contains a subset $C_+ \subset L_+$ of points representing convex 8-gons. Even if a point starts out representing a convex

4

polygon, the torus motion eventually moves the point outside the region where it is convex – unless it is Poncelet to begin with.

Figure 2 (right) shows a planar projection of the first $2^{19}$ points of an orbit that does not contain points representing convex 8-gons. This orbit appears to lie on a higher genus surface with a singular flat structure. This kind of orbit is not relevant for our analysis but it makes a beautiful picture and hints at some additional structure to be explored.

An earlier and more complicated version of this paper actually showed that the metric completions of orbits like the one shown on the left in Figure 2 are flat tori. However, when revising the paper, I found a shorter proof which only requires an analysis of the pair $(C_+, L_+)$. I thought that the torus result was pretty, but it seems to me that the new proof is much more likely to generalize.

This paper is organized as follows. In §2 I will prove Theorem 1.4. In §2.9 I give a 6-step outline of the proof of the Main Theorem. The rest of the paper carries out the steps of the outline.

The interested reader can download the computer program I wrote, which does experiments with the 3-diagonal map on $\mathcal{P}_{8,2}$. See
**http://www.math.brown.edu/∼res/Java/OCTAGON.tar**

## 1.1   Acknowledgements

# 2 The Main Ideas

## 2.1 Complete Integrability

We begin with a quick introduction to integrable systems.

Let $V$ be an open subset of $\mathbf{R}^4$. Let $F_1, F_2 : V \to \mathbf{R}$ be smooth functions. The pair $(x_1, x_2) \in \mathbf{R}^2$ is a *regular value* if the following is true: For all $p \in V$ such that $F_1(p) = x_1$ and $F_2(p) = x_2$, the gradients $\nabla F_1$ and $\nabla F_2$ are nonzero and linearly independent. In this case, $\Sigma = F_1^{-1}(x_1) \cap F_2^{-1}(x_2)$ is a smooth surface. We call such a $\Sigma$ a *regular level set*.

Now suppose $\omega$ is a symplectic form on $V$ – i.e., a closed and nondegenerate 2-form. There is a unique vector field $X_j$ such that $\omega(X_j, V) = D_V F_j$. Here $D_V F_j$ is the directional derivative of $F_j$ in the direction of $V$. The vector field $X_j$ is called the *Hamiltonian vector field* associated to $F_j$. Because $\omega(X_j, X_j) = 0$, the vector field $X_j$ is tangent to the level set of $F_j$. Also, the flow generated by $F_j$ preserves $\omega$.

The functions $F_1$ and $F_2$ *Poisson commute* if $\omega(X_1, X_2) = 0$ everywhere. The vectors $X_1, X_2$ are linearly independent at some point iff the gradients $\nabla F_1, \nabla F_2$ are linearly independent at this point. When this happens, the restriction of $\omega$ to a regular level set $\Sigma$ is 0. That is, $\Sigma$ is *Lagrangian*. The vector fields $X_1$ and $X_2$ define commuting flows preserving both $\Sigma$ and $\omega$.

We can use the commuting flows to define coordinate charts from $\Sigma$ into $\mathbf{R}^2$ in a canonical way. We start with some point $p \in \Sigma$, which we map to the origin. Each point $q \in \Sigma$ sufficiently near to $p$ defines two numbers $a_1(p, q)$ and $a_2(p, q)$ such that one can reach $q$ by starting at $p$ and flowing for time $a_1(p, q)$ along $X_1$ and then for time $a_2(p, q)$ along $X_2$. The coordinate chart is given by $q \to (a_1(p, q), a_2(p, q))$. The commuting nature of the flows combines with the linear independence to show that this map really is a local coordinate chart about $p$. By construction, the overlap functions for our coordinate chart are translations. Thus $\Sigma$ has the structure of translation surface (without singular points).

Let us combine all this with dynamics. Let $U \subset V \subset \mathbf{R}^4$ be two open sets and suppose we have a smooth map $T : U \to V$. Suppose that all of $\omega, F_1, F_2$ are $T$-invariant. Then $T(\Sigma \cap U) \subset \Sigma$, and $T : \Sigma \cap U \to \Sigma$ is a translation in these coordinates. In this case we would call $T$ *completely integrable* with respect to the pair $(U, V)$.

In our case, $T$ is a rational map, and $\omega, F_1, F_2$ will be defined in terms of rational functions. All these objects have singularities; they are only defined on open dense subsets of $\mathbf{R}^4$. However, we will always restrict our attention to suitable pairs $(U, V)$ of open sets where everything is everywhere defined.

## 2.2 The Map in Coordinates

Every member $P \in \mathcal{P}_{8,2}$ has a canonical representative with vertices

$$(1,0), \ (a,b), \ (0,1), \ (-d,c), \ (-1,0), \ (-a,-b), \ (0,-1), \ (d,-c). \qquad (1)$$

We label these vertices $v_0, ...., v_7$. We call $p = (a,b,c,d)$ the *coordinates* of $P$. When $(a,b) = (c,d)$ our point lies in the space $\mathcal{P}_{8,4}$ of affine equivalence classes of 8-gons with 4-fold rotational symmetry.

When we apply the map $T_3$ we initially get a polygon $P'$ with vertices $v'_0, ..., v'_7$, where

$$v'_k = \overline{v_{k+1}v_{k+4}} \cap \overline{v_{k+2}v_{k+5}},$$

where the indices are taken mod 8. Then we normalize to get back to Equation 1 and find the new coordinates $(a', b', c', d') = T_3(a,b,c,d)$. One could use other labeling conventions, but this one leads to a nice formula for $T_3$. Let $e = ac + bd$.

$$T_3 = A\Delta A\Delta, \qquad (2)$$

$$A(a,b,c,d) = (-b, -a, -d, -c), \qquad (3)$$

$$\Delta = \left( \frac{b(c+d+1)}{c(e+a+c+1)}, \frac{d(e+b+c)}{c(e+a+c+1)}, \frac{d(a+b+1)}{a(e+a+c+1)}, \frac{b(e+a+d)}{a(e+a+c+1)} \right) \qquad (4)$$

The map $\Delta$ is nice because all its component functions are positive.

We note some useful symmetries. We let $\sqrt{I}$ denote the map we get by replacing the polygon in Equation 1 by the index-shifted polygon

$$(a,b), (0,1), (-d,c), (-1,0), (-a,-b), (0,-1), (d,-c), (1,0)$$

and then renormalizing as in Equation 1. The map $I = \sqrt{I} \circ \sqrt{I}$ has a simpler formula. We let $J$ be the map which reflects the polygon in the line $y = x$ and then dihedrally relabels the coordinates so that the polygon starts out $(1,0), (b,a), ....$ In coordinates, we have

$$\sqrt{I}(a,b,c,d) = \left( \frac{d}{e}, \frac{a}{e}, \frac{b}{e}, \frac{c}{e} \right),$$

$$I(a,b,c,d) = (c,d,a,b)$$

$$J(a,b,c,d) = (b,a,d,c). \qquad (5)$$

We have

$$\sqrt{I}T_3 = T_3\sqrt{I}, \qquad IT_3 = T_3I, \qquad JT_3J = IT_3 \qquad JT_3^2 = T_3^2J \qquad (6)$$

## 2.3  Some Important Functions

Let $\mathcal{I} \subset \mathcal{P}_{8,2}$ denote the subset consisting of equivalence classes of 8-gons which are inscribed in a conic section. Let $\mathcal{I}^* \subset \mathcal{P}_{8,2}$ denote the subset consisting of equivalence classes of 8-gos circumscribed about a conic section. Define functions

$$g_{ab}^* = a - b, \qquad g_{cd}^* = c - d, \qquad g_{ab} = \frac{1 - a^2 - b^2}{ab}, \qquad g_{cd} = \frac{1 - c^2 - d^2}{cd}. \tag{7}$$

A computation shows that

$$(a, b, c, d) \in \mathcal{I} \iff g_{ab} + g_{cd} = 0, \quad (a, b, c, d) \in \mathcal{I}^* \iff g_{ab}^* + g_{cd}^* = 0. \tag{8}$$

The first of these equations has a simple geometric interpretation. From the way we have normalized our 8-gons, the point $(a, b)$ lies on the ellipse $x^2 + y^2 + g_{ab}xy = 1$. The point $(-d, c)$ lies on the ellipse $x^2 + y^2 - g_{cd}xy = 1$. If these points lie on the same ellipse then the constants are the same, meaning that $g_{ab} + g_{cd} = 0$. I don't know a nice geometric interpretation for the second equation, but it is an easy calculation. Define

$$G(a, b, c, d) = 2(g_{ab} + g_{cd})(g_{ab}^* + g_{cd}^*). \tag{9}$$

**Discussion:** (The reader can safely ignore this.) Motivated by Equation 8 I guessed that $G$ is a $T_3$ invariant. Motivated by the literature on the pentagram map, e.g. my paper [19], I then guessed that the polynomial expression $(O_8/E_8)^{1/6}$ is also a $T_3$ invariant. The functions $O_8$ and $E_8$ are (now) called the *odd and even Casimirs* for the $T_2$-invariant Poisson structure. Fooling around, I came up with algebraically nicer ones, $F_1$ and $F_2$, described in the next section. The invariants $F_1$ and $F_2$ satisfy the relations:

$$F_2 - F_1 = G, \qquad \frac{F_1}{F_2} = (O_8/E_8)^{1/6}. \tag{10}$$

According to the anonymous referee, the invariants $F_1$ and $F_2$ can be interpreted in terms of previous work [5], [7] on $T_3$. In [5], it is shown that there is a (non-invertible) map $\Phi$ from planar polygons to corrugated polygons in $\boldsymbol{RP}^3$ which intertwines $T_3$ with the analogous map on corrugated polygons. Pulling back an invariant for corrugated polygons gives an invariant of $T_3$ on ordinary polygons. Moreover the invariants for $T_3$ on corrugated polygons can be deduced from the Lax pair in [7]. One can interpret a centrally symmetric octagon as a quadrilateral whose monodromy has eigenvalues $(-1, -1, 1)$. Applying $\Phi$ we get a corrugated quadrilateral whise monodromy has eigenvalues $(1, -1, 1, \mu)$. The quantity $1/\mu$ is precisely $F_1/F_2$, and the monodromy is an invariant.

## 2.4 Proof of Theorem 1.4

Let $e = ac + bd$. Our two basic invariants for $T_3$ are $F_1$ and $F_2$ where

$$F_1 = \frac{(1+a-b)(1+c-d)(e+b-c)(e+d-a)}{abcd},$$

$$F_2 = \frac{(1-a+b)(1-c+d)(e-b+c)(e-d+a)}{abcd}. \tag{11}$$

Referring to the maps in Equation 5, these functions obey the symmetries: $F_j \circ I = F_j$ and $F_{3-j} = F_j \circ J$. One can calculate in Mathematica directly that $F_1$ and $F_2$ are invariants for $A$ and for $\Delta$, and hence for $T_3$. One evaluation suffices to check that $\nabla F_1$ and $\nabla F_2$ are linearly independent at some point/ Hence $F_1$ and $F_2$ are algebraically independent.

The invariant symplectic form is.

$$\omega = \frac{1}{ab}\mathbf{d}a \wedge \mathbf{d}b + \frac{1}{cd}\mathbf{d}c \wedge \mathbf{d}d. \tag{12}$$

One can see directly that $A^*(\omega) = -\omega$. We will describe the calculation that shows $\Delta^*(\omega) = -\omega$. The two facts together imply that $\omega$ is $T_3$ invariant. Let $e_1, e_2, e_3, e_4$ be the standard basis vectors on $\mathbf{R}^4$. Let $\Psi$ denote the Jacobian of $\Delta$, namely the $4 \times 4$ matrix of partial derivatives. (To avoid mixing up the matrix with its transpose, let me say that the first column is $\partial\Delta/\partial a$, and the second column is $\partial\Delta/\partial b$, etc.) Let

$$(a', b', c', d') = \Delta(a, b, c, d).$$

We compute

$$\Delta^*(\omega)(e_i, e_j) =$$

$$\frac{1}{a'b'}(\Psi_{1i}\Psi_{2j} - \Psi_{2i}\Psi_{1j}) + \frac{1}{c'd'}(\Psi_{3i}\Psi_{4j} - \Psi_{4i}\Psi_{3j}) =^{(!)}$$

$$-\omega(e_i, e_j). \tag{13}$$

The equality with an exclaimation point is, for each $(i, j)$, a big Mathematica calculation that miraculously works out.

Given the simple nature of $\omega$ we can write down the Hamiltonian vector field $X_\phi$ for a function $\phi : \mathbf{R}^4 \to \mathbf{R}$ in an explicit way. We have

$$X_\phi = (-ab\phi_b, ab\phi_a, -cd\phi_d, cd\phi_c). \tag{14}$$

Here $\phi_a = \partial\phi/\partial a$, etc. $X_\phi$ is defined wherever $\phi$ is.

Let $X_j$ be the Hamiltonian vector field associated to $F_j$. Another Mathematica calculation shows that $\omega(X_1, X_2) = 0$. Now we have established all the points of Theorem 1.4.

9

## 2.5 Positivity

Let $\mathcal{C}$ be the set of points representing convex 8-gons without 4-fold rotational symmetry. So, we are throwing out points of the form $(a, b, a, b)$.

**Lemma 2.1 (Positivity)** *All factors of $F_1$ and $F_2$ are positive on $\mathcal{C}$.*

**Proof:** Let $(a, b, c, d) \in \mathcal{C}$. The convexity gives the constraints

$$a, b, c, d > 0, \quad |a - b| < 1, \quad |c - d| < 1, \quad a + b > 1, \quad c + d > 1.$$

Let $e = ac + bd$, as in the definition of $F_1$ and $F_2$. To finish the proof we just need to show that the 4 quantities $e + b - c$ and $e - b + c$ and $e + a - d$ and $e + d - a$ are positive. By symmetry it suffices to show $e + b - c > 0$:

$$e + b - c = ac + bd + b - c = (a - 1)c + bd + b > -bc + bd + b = b(d - c + 1) > 0.$$

The first inequality comes from $a + b > 1$ and the second from $d - c > -1$. ♠

**Lemma 2.2** $(a, b, c, d) \in \mathcal{C} - \mathcal{I} - \mathcal{I}^*$ *lies on one of four connected components of $\mathcal{C}$, depending only on the signs of $g_{ab} + g_{cd}$ and $g_{ab}^* + g_{cd}^*$.*

**Proof:** Let $\mathcal{C}'$ denote the set of all points $(a, b, c, d)$. The set $\mathcal{C}' - \mathcal{C}$ is a 2-dimensional set where $(a, c) = (b, d)$. This set does not disconnect $\mathcal{C}'$. Thus, it suffices to prove our result for $\mathcal{C}'$ rather than $\mathcal{C}$. We claim that the map

$$\psi(a, b, c, d) = (g_{ab}, g_{cd}, g_{ab}^*, g_{cd}^*) = (a', b', c', d')$$

is a homeomorphism – indeed a diffeomorphism – from $\mathcal{C}'$ to the rectangular solid $Q = (-2, 2)^2 \times (-1, 1)^2$. By Equation 8, $\psi$ maps $\mathcal{I}$ and $\mathcal{I}^*$ respectively into the hyperplanes $H$ and $H^*$ given by $a' + b' = 0$ and $c' + d' = 0$. The 4 components of $\mathcal{C}' - \mathcal{I} - \mathcal{I}^*$ are the images of $\psi^{-1}$ of the 4 components of $Q - H - H^*$.

For the homeomorphism claim, it suffice to prove the simpler result that the map

$$(a', c') = \left( \frac{1 - a^2 - b^2}{ab}, a - b \right).$$

is a homeomorphism onto $(-2, 2) \times (-1, 1)$ from set of $(a, b)$ such that $a, b > 0$ and $|a - b| < 1$ and $a + b > 1$. The reason is that $a'$ is the determining coefficient of the ellipse through the points $(\pm 1, 0)$ and $(0, \pm 1)$ containing $(a, b)$ – see the geometric interpretation of $g_{ab}$ given in §2.3 – and $c'$ selects the ray of slope 1, emenating from the line $x + y = 1$, which contains $(a, b)$. ♠

## 2.6 Duality and Convexity

In this section we prove the following result

**Lemma 2.3** *The map $A\Delta A$ maps $\mathcal{C}$ into itself and preserves the component on which $g_{ab} + g_{cd}$ and $g_{ab}^* + g_{cd}^*$ are positive.*

**Proof:** Our proof gives an interpretation of $\iota_3 = A\Delta A$ as implementing projective duality. Here is how one represents the line through $p_1 = (x_1, y_1)$ and $p_2 = (x_2, y_2)$.

1. We move to the affine patch in $\boldsymbol{R}^3$ by setting $v_j = (x_j, y_j, 1)$.

2. We take the cross product $w = v_1 \times v_2 = (w_1, w_2, w_3)$.

3. We move back to the plane by setting $[p_1, p_2] = (w_1/w_3, w_2/w_3)$.

Concretely, the new point is

$$[p_1, p_2] = \left( \frac{y_1 - y_2}{x_1 y_2 - x_2 y_1}, \frac{x_2 - y_1}{x_1 y_2 - x_2 y_1} \right). \tag{15}$$

Given the polygon $P$ in Equation 1, with successive points $P_1, P_2, ...$ we define

$$P^* = [P_1, P_2], [P_2, P_3], [P_3, P_3], [P_4, P_5], ... \tag{16}$$

We then normalize by the needed affine transformation so that the polygon starts out $(1, 0), (a^*, b^*), (0, 1), (-d^*, c^*), ...$ We write

$$\iota_3^*(a, b, c, d) = (a^*, b^*, c^*, d^*). \tag{17}$$

The dual of a convex octagon is again convex. Hence $\iota_3^*$ maps points representing convex octagons to points representing convex octagons. We check that $\iota_3^*(a, b, a, b) = (a^*, b^*, a^*, b^*)$, so that $\iota_3^*$ preserves octagons with 4-fold rotational symmetry.

Here is the punchline. We compute that

$$\iota_3 = \iota_3^* \circ I \circ J. \tag{18}$$

Thus $\iota_3$ is the composition of maps which all preserve $\mathcal{C}$.

Finally, $\iota_3^*$, being a coordinatization of duality, swaps the sets $\mathcal{I}$ and $\mathcal{J}$. Hence, so does $\iota_3$. But then $\iota_3$ permutes the 4 components from Lemma 2.2. A single suffices to check that $\iota_3$ preserves the $(+, +)$ component. ♠

**Remark:** One could prove all this algebraically, but it is rather messy.

11

## 2.7 Integral Curves

Let $X_G = X_2 - X_1$ be the Hamiltonian vector field associated to $G = F_2 - F_1$. We let $\mathcal{X}$ denote the set of $(a, b, c, d)$ such that

1. $a, b, c, d$ are all nonzero.

2. $F_1, F_2, G$ are all nonzero. So, $1 \pm a \mp b$ and $1 \pm c \mp d$ are nonzero.

3. $(a, b) \neq (c, d)$. We are throwing out the points corresponding to $\mathcal{P}_{8,4}$.

**Lemma 2.4** *In each connected component of $\mathcal{X}$ we can find a smooth function $\zeta$ such that $X_G \cdot \nabla \zeta \neq 0$. In particular, $X_G$ never vanishes on $\mathcal{X}$.*

**Proof:** Recall that $G = 2(g_{ab}^* + g_{cd}^*)(g_{ab} + g_{cd}) \neq 0$ on $\mathcal{X}$. When $ac/bd > 0$ we define $h = \log(ac/bd)$. We compute

$$X_G \cdot \nabla g_{ab}^* = 2(g_{ab}^* + g_{cd}^*)(1 - a + b)(1 + a - b)(a + b)/(ab). \qquad (19)$$

$$X_G \cdot \nabla g_{cd}^* = 2(g_{ab}^* + g_{cd}^*)(1 - c + d)(1 + c - d)(c + d)/(cd). \qquad (20)$$

$$X_G \cdot \nabla g_{ab} = -2(g_{ab} + g_{cd})(1 - a + b)(1 + a - b)(a + b)/(ab). \qquad (21)$$

$$X_G \cdot \nabla g_{cd} = -2(g_{ab} + g_{cd})(1 - c + d)(1 + c - d)(c + d)/(cd). \qquad (22)$$

$$X_G \cdot \nabla h = 2(g_{ab}^* + g_{cd}^*)\big((1 + a^2 + b^2)/(ab) + (1 + c^2 + d^2)/(cd)\big). \qquad (23)$$

Now we observe the following about a component $\mathcal{U}$ of $\mathcal{X}$.

1. If $ab > 0$ in then $a + b \neq 0$. We can take either $\zeta = g_{ab}$ or $\zeta = g_{ab}^*$.

2. If $cd > 0$ in then $c + d \neq 0$. We can take either $\zeta = g_{cd}$ or $\zeta = g_{cd}^*$.

3. If $ab < 0$ and $cd < 0$ then $h$ is defined in $\mathcal{U}$ and we can take $\zeta = h$.

In all cases we have the desired function. ♠

Say that a *G-curve* is a maximal curve tangent to $X_G$. Lemma 2.4 says that $\mathcal{X}$ is foliated by $G$-curves and that each $G$-curve $\gamma$ exits every compact subset of $\mathcal{X}$ at both ends. Why? Because $\zeta$ from Lemma 2.4 (which depends on the component of $\mathcal{X}$ that contains $\gamma$) is monotone along $\gamma$.

Lemma 2.4 has an immediate consequence: At every point of $\mathcal{X}$, at least one of the vector fields $X_1$ or $X_2$ is nonzero. This comes from the fact that $X_G = X_2 - X_1$ is nonzero at each point of $\mathcal{X}$. This result is not such a strong result. We will be very interested in showing systematically that $X_1$ and $X_2$ are actually linearly independent at certain points of $\mathcal{X}$. As we mentioned at the end of the introduction, an appeal to Sard's theorem will not be good enough for our purposes.

## 2.8 The Dependence Set

It would be nice to prove, simply, that the two vectorfields $X_1$ and $X_2$ are linearly independent at each point of $\mathcal{X}$. Unfortunately, this is not quite true. These vector fields are linearly dependent on a certain set $\mathcal{Y}$ defined by the equations:

$$ac + bd + 1 = ac^2 + ca^2 + bd^2 + db^2 = 0. \tag{24}$$

I found this doing the analysis for Case 9 in the next chapter.

Recall that $T_3 = A\Delta A\Delta$. The set $\mathcal{Y}$ is clearly $A$-invariant. One can also give a tedious algebraic proof that $\mathcal{Y}$ is $\Delta$-invariant and hence $T_3$-invariant. Rather than do this, let me give a *post hoc* proof. We will prove in the next chapter that $\mathcal{Y}$ is precisely the locus in $\mathcal{X}$ where the vector fields $X_1$ and $X_2$ are linearly dependent. Since the action of $\Delta$ preserves this property, we see that $\mathcal{Y}$ is $\Delta$-invariant. I don't have a geometric interpretation of $\mathcal{Y}$.

The set $\mathcal{Y}$ does bother us because it is disjoint from the level sets of interest to us. I will now show that $F_1$ and $F_2$ are never both positive on $\mathcal{Y} \cap \mathcal{X}$. After a lot of trial and error I found the polynomial.

$$Y(x_1, x_2) = 512 + 216x_1x_2 + 192(x_1 + x_2) - 30(x_1 + x_2)^2 + (x_1 + x_2)^3. \tag{25}$$

**Lemma 2.5** $Y(F_1, F_2) = 0$ *for points in* $\mathcal{Y} \cap \mathcal{X}$.

**Proof:** Solving $ac + bd + 1 = 0$ we get $d = (-ac - 1)/b$. When we make this substitution we get the equation

$$Y(F_1(a, b, c, d), F_2(a, b, c, d)) = \frac{\phi_1 \phi_2}{(abcd)^3}$$

where

$$\phi_1 = b^2(ac^2 + ca^2 + bd^2 + db^2)$$

and $\phi_2$ is a messy polynomial we don't care about. Since $\phi_1 = 0$ on $\mathcal{Y}$ and $abcd$ is nonzero on $\mathcal{X}$, we see that $Y(F_1, F_2) = 0$ on $\mathcal{Y} \cap \mathcal{X}$. ♠

**Lemma 2.6** $Y(x_1, x_2) > 0$ *when* $x_1, x_2 > 0$.

**Proof:** We compute that $\partial Y/\partial x_1 + \partial Y/\partial x_2 = 6(8 + x_1 + x_2)^2 > 0$. So, if this lemma is false, then $Y$ is negative somewhere on the positive $x$-axis. We have $Y(x, 0) = (x + 2)(16 - x)^2 \geq 0$ on the positive $x$-axis. Hence $Y > 0$ when $x_1, x_2 > 0$. ♠

## 2.9 Proof of the Main Theorem: Outline

**Step 1, Linear Independence:** Let $\mathcal{X}_+ \subset \mathcal{X}$ denote the subset where all factors of $F_1, F_2, G$ (both the in the numerator and in the denominator) are positive. For instance $a, b, c, d > 0$ and $g_{ab} + g_{cd} > 0$ and $1 + a - b > 0$ on $\mathcal{X}_+$. In particular $F_1, F_2, G > 0$ on $\mathcal{X}_+$. In §3 we prove that $X_1$ and $X_2$ are linearly independent at every point of $\mathcal{X} - \mathcal{Y}$, which implies that they are linearly independent at every point of $\mathcal{X}_+$.

**Step 2, The Cylinder and the Nice Loop:** Let $L_+$ be a level set in $\mathcal{X}_+$. Let $\mathcal{U}$ denote the set $(a, b, c, d)$ where $a, b, c, d > 0$ and $\max(a+b, c+d) = 1$. In §4, we prove that every $G$-curve in $L_+$ intersects $\mathcal{U}$ exactly once, and that $L_+ \cap \mathcal{U}$ is a single loop which we call the *nice loop*. The nice loop is smooth away from the 2 points on it satisfying $a + b = c + d = 1$. From all this we deduce that $L_+$ is a cylinder. For points in $\mathcal{P}_{8,4}$, treated in [21], the set $L_+$ is an arc: a single $G$-curve.

**Step 3, Intrinsic Boundedness and Concavity:** In §5 we prove that each level set $L_+$ in $\mathcal{X}_+$ is bounded with respect to its intrinsic flat structure coming from its integrability. We also prove that $L_+$ is locally concave near its intrinsic boundary by showing that $\iota_5 = A\Delta A\Delta A$ is an isometry of the sub-cylinder $L'_+ \subset L_+$ bounded by the nice loop and the end of $L_+$ which abuts $(0, 0, 0, 0)$. The map $\iota_5$ swaps the ends of $L'_+$ and thus allows us to convert info about the nice loop into info about one end of $L_+$. We prove $\Delta$ preserves $L_+$ and swaps its ends. This gives us info about the other end of $L_+$. What we are saying is that we use various maps in the semigroup $\langle A, \Delta \rangle$ to convert information that we can get from looking at the interior of $\mathcal{X}_+$ to information about the ends of our level sets.
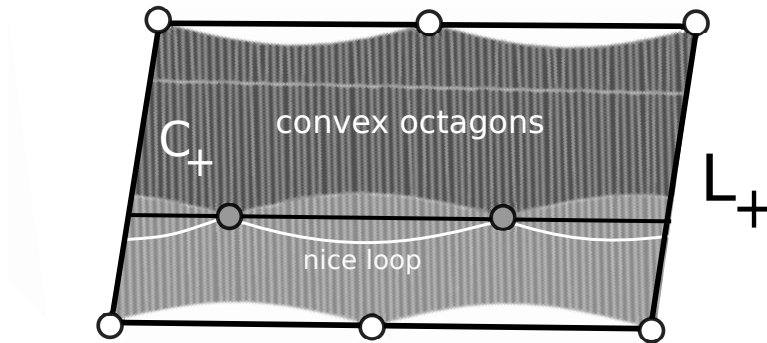


Figure 3: The geometry of $L_+$ and $C_+$ when $F_1 = 7/2$ and $F_2 = 4$.

Figure 3 shows a plot of the cylinder $L_+$ when the invariants are $F_1 = 7/2$ and $F_2 = 4$. I picked these values somewhat arbitrarily. The left and right sides are meant to be identified. My program draws a chunk of the universal cover of $L_+$ (by numerically integrating various of the Hamiltonian vector fields) and then I am cutting off the picture by taking a fundamental domain. The top and bottom horizontal lines contain the lifts of the cusp points to the planar universal cover. Given the symmetry $I$ from Equation 5, which is an isometry of $L_+$ and which permutes the two cusp points, we see that indeed there is a straight line which contains the cusps on the top boundary and likewise on the bottom.

The darkly shaded region is the set $C_+ = L_+ \cap \mathcal{C}$. This set is not always a cylinder, though it is in some cases. In all cases, it lies on one side of the nice loop and touches the nice loop at the two cusp points of the nice loop. The light curve in Figure 3 is a hand-drawn approximation of the nice loop.

We say that the *top line* is the straight line through the cusps of the cylinder end that lies on the same side of the nice loop as $C_+$. We say that the *bottom line* is the line through the cusps on the other end of $L_+$. Thus $L_+$ determines 2 parallel straight lines, the top line and the bottom line. We say that the *middle line* is the line through the cusps on the nice loop. The concavity of the boundary and the properties of the nice loop will imply that the middle line is strictly between the top and bottom lines.

**Step 4: The Invariant and the Yardstick:** We fix a flat metric on $L_+$ and then work with a planar isometric copy of $L_+$ as in Figure 3 above and (the copied) Figure 4 below.
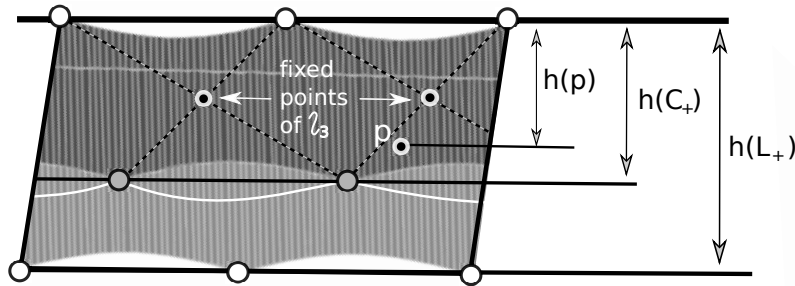


Figure 4: The quantities $h(p)$ and $L(C_+)$ and $h(L_+)$.

We let $h(L_+)$ be the distance between the top and bottom lines. Essentially $h(L_+)$ is the height of $L_+$. Let $h(C_+)$ denote the distance between the top and middle lines. Once we show that the middle line lies strictly between the top and bottom lines, we have $h(C_+) < h(L_+)$. Given $p \in L_+$

we define $\ell(p)$ to be the line through $p$ parallel to the top, bottom, and middle lines, and then we define $h(p)$ to be the distance between the top line and $\ell(p)$. We then introduce the following quantities:

$$\lambda(L_+) = 1 - \frac{h(C_+)}{h(L_+)} \qquad \lambda(p) = \frac{h(p)}{h(L_+)}. \qquad (26)$$

Any two flat metrics on $L_+$ are affinely equivalent, so $\lambda(L_+)$ is a function of our invariants $F_1$ and $F_2$. The quantity $\lambda(p)$ is also independent of the choice of flat structure and thus a function of $p$.

**Step 5: The Magic Formula:** We will see that the order 2 isometry $\iota_3$ swaps the top and middle lines, and the order 2 isometry $\Delta$ swaps the top and bottom lines. For this reason, we have

$$\lambda(T_3(p)) = \lambda(p) - \lambda(C_+), \qquad \lambda(T_3^{-1}(p)) = \lambda(p) + \lambda(C_+). \qquad (27)$$

The first equation is valid as long as $p, T_3(p) \in L_+$. The second is valid as long as $p, T_3^{-1}(p) \in L_+$. Equation 27 implies that at most $\lambda(p)/\lambda(L_+)$ forward iterates of the octagon $O_p$ represented by $p$ are convex. After that, they must exit $L_+$. Likewise, at most $(1 - \lambda(p))/\lambda(L_+)$ iterates of $O_p$ under $T_3^{-1}$ are convex. Either one of these statements establishes Theorem 1.1 for all centrally symmetric octagons represented by points in $\mathcal{X}_+$.

Call an octagon *convex generic* if it is convex, and neither inscribed nor circumscribed, and without 4-fold rotational symmetry. If Theorem 1.1 has a counter-example $p$ which is generic convex then, as we show, we can apply some element $\gamma$ in the group generated by the maps $\sqrt{I}$ and $J$ so that $\gamma(p)$ is represented by a point in $\mathcal{X}_+$. Then $\gamma(p)$ would also be a counter-example. This proves Theorem 1.1 in the generic convex case. The case of 4-fold symmetry follows from [21].

Let mention one more consequence of Equation 27. For any convex octagon $O_p$ represented by $p \in L_+$, we can look at the picture we get, as in Figure 1, by iterating $T_3$ both forwards and backwards. At most $1/\lambda(L_+)$ steps of the picture around $O_p$ can be convex.

**Step 6, Inscribed and Circumscribed Cases:** In §7 we show that $\mathcal{I}^*$ is foliated by invariant sets which (when completed) are holomorphically equivalent to the Riemann sphere. Under this equivalence, the map $T_3$ acts as a hyperbolic linear fractional transformation. The attracting fixed point in each level set is convex Poncelet and the repelling fixed point is the star-reordering of the attracting fixed point. This establishes Theorem 1.3 and all the statements of Theorem 1.2 pertaining to 8-gons in $\mathcal{I} \cup \mathcal{I}^*$.

# 3  Linear Independence

## 3.1  Resultants

In this chapter we carry out Step 1 of the outline given in §2.9. Our proof is very algebraic, and we begin with a discussion of resultants.

The resultant of $P = a_2 x^2 + a_1 x + a_0$ and $Q = b_3 x^3 + b_2 x^2 + b_1 x + b_0$ is the number

$$\mathrm{res}(P, Q) = \det \begin{bmatrix} a_2 & a_1 & a_0 & 0 & 0 \\ 0 & a_2 & a_1 & a_0 & 0 \\ 0 & 0 & a_2 & a_1 & a_0 \\ b_3 & b_2 & b_1 & b_0 & 0 \\ 0 & b_3 & b_2 & b_1 & b_0 \end{bmatrix} \tag{28}$$

This vanishes if and only if $P$ and $Q$ have a common (complex) root. The case for general polynomials is simliar; see §2 of [24].

In the multivariable case, one can treat two polynomials $P(x_1, ..., x_n)$ and $Q(x_1, ..., x_n)$ as elements of the ring $R[x_n]$ where $R = \boldsymbol{C}[x_1, ..., x_{n-1}]$. The resultant $\mathrm{res}_{x_n}(P, Q)$ computes the resultant in $R$ and thus gives a polynomial in $\boldsymbol{C}[x_1, ..., x_{n-1}]$. The polynomials $P$ and $Q$ simultaneously vanish at $(x_1, ..., x_n)$ only if $\mathrm{res}_{x_n}(P, Q)$ vanishes at $(x_1, ..., x_{n-1})$.

## 3.2  The Proof modulo the Non-Vanishing Lemma

Let $\mathcal{D}$ be the subset of $\mathcal{X}$ where $X_1$ and $X_2$ are linearly dependent. We want to show that $\mathcal{D} = \mathcal{Y}$, the set defined by Equation 24. We compute that the following expression is an integer polynomial, and by definition it vanishes identically on $\mathcal{D}$.

$$f = \frac{abc^2 d^2 (X_{11} X_{22} - X_{21} X_{21})}{2(1 - a + b)(1 - b + a)(1 - c + d)(1 + c - d)}. \tag{29}$$

Here $X_{ij}$ is the $j$th component of $X_i$.

A calculation – compare Lemma 2.4 – shows that $X_G \cdot \mu = 0$, where $\mu = (\alpha, -\alpha, -\beta, \beta)$ and

$$\alpha = ab(c + d)(1 + c - d)(1 + d - c), \qquad \beta = cd(a + b)(1 + a - b)(1 + b - a).$$

When $X_1$ and $X_2$ are linearly dependent they are both multiples of $X_G$. Hence $X_1 \cdot \mu = X_2 \cdot \mu = 0$ on $\mathcal{D}$. We compute that

$$g = \frac{abcd(X_1 \cdot \mu)}{(1 - a + b)(1 - b + a)(1 - c + d)(1 + c - d)} \tag{30}$$

is an integer polynomial, and it vanishes identically on $\mathcal{D}$. We compute

$$h := \operatorname{res}_a(f, g) = \phi_1 \phi_2 \phi_3 \phi_4 \phi_5^2 \phi_6 \phi_7^2 \phi_8^2 \phi_9. \qquad (31)$$

Where $\phi_1, ..., \phi_9$ are, in order, the functions

$$b - 1 \qquad b + 1 \qquad b - c \qquad b - d \qquad c + d \qquad bc + bd + cd - c^2$$

$$b\text{--}c\text{+}bc\text{--}bd\text{--}cd\text{--}c^2 \qquad \text{--}b\text{+}c\text{+}bc\text{--}bd\text{--}cd\text{--}c^2 \qquad c(bd^2\text{+}db^2)\text{+}(bd\text{+}1)(bd\text{+}1\text{--}c^2). \quad (32)$$

One important point we note that is that the flow generated by $X_G$ is a symplectomorphism which preserves $F_1, F_2$. Hence $\mathcal{D}$ is foliated by $G$-curves. We say $\phi_j$ is *bad* if it vanishes on a nontrivial arc of a $G$-curve that lies in $\mathcal{X} - \mathcal{Y}$, and otherwise *good*. Below we will prove:

**Lemma 3.1 (Non-Vanishing)** *The functions $\phi_1, ..., \phi_9$ are all good.*

Since $f$ and $g$ vanish identically on $\mathcal{D}$, the resultant $h$ also vanishes identically on points $(b, c, d)$ such that $(a, b, c, d) \in \mathcal{D}$ for some choice of $d$. Suppose now that there exists a point $p \in \mathcal{D} - \mathcal{Y}$. Then there is an entire $G$-curve $\gamma$ in $\mathcal{D} - \mathcal{Y}$. By the Non-Vanishing Lemma, each $\phi_j$ is nonzero on an open dense subset of $\gamma$. But then all $\phi_j$ are nonzero on the (open dense) intersection of these 9 open dense sets. In particular, we can find a point $(a, b, c, d) \in \mathcal{D}$ where $h(b, c, d) \neq 0$. This contradiction finishes the proof.

### 3.3 Proof of the Non-Vanishing Lemma

Given rational functions $\psi_1$ and $\psi_2$ we let $\psi_1^*$ and $\psi_2^*$ respectively be the numerator and denominator of $\psi_1/\psi_2$ when this is in lowest terms.

**Cases 1 and 2:** If $\phi_1 = b - 1$ is bad, then $b = 1$ and $X_2 \cdot (0, 1, 0, 0) = 0$. The only nonzero solution is

$$a = \frac{1 + c - d}{2c}. \qquad (33)$$

We set $a$ as in Equation 33 then compute that $\operatorname{res}_c(f^*, g^*)$ and $\operatorname{res}_d(f^*, g^*)$ are nontrivial 1-variable polynomials respectively in $d$ and $c$. This means that $f^*$ and $g^*$ only vanish for finitely many pairs $(c, d)$. The ratios $f/f^*$ and $g/g^*$ have the form $c^i(1 + c - d)^j$ and do not vanish. Hence $f$ and $g$ only vanish at finitely many points in $\mathcal{X}$ with $b = 1$ and $a$ as in Equation 33. This is a contradiction. Hence $\phi_1$ is good. $\phi_2$ is good by symmetry: The map $p \to -p$ carries $\phi_1$ to $\phi_2$ and preserves $\mathcal{D}, \mathcal{X}, \mathcal{Y}$.

**case 3:** Suppose that $\phi_3 = b - c$ is bad. Then we have $b = c$ and

$$X_G \cdot (0, 1, -1, 0) = 4(a + d)(a - d) = 0.$$

Hence $a = \pm d$. In either case we compute $G(a, b, b, \pm a) = 0$ so our point does not lie in $\mathcal{X}$. This contradiction shows that $\phi_3$ is good.

**Case 4:** Suppose $\phi_4 = b - d$ is bad. We have $d = b$ and

$$0 = X_G \cdot (0, 1, 0, -1) = \frac{4(a - c)(a - b + c)(ac + b^2 - 1)}{ac}$$

If $a = c$ then $(a, b, a, b) \notin \mathcal{X}$. If $a = (1 - b^2)/c$ we compute $G(a, b, c, b) = 0$. Again, our point does not lie in $\mathcal{X}$. Hence $a = b - c$. The rest of the proof is like Case 1 except that we use the $b$ and $c$ variables for the resultants. This time $f/f^*$ and $g/g^*$ both have the form $b^i(b - 2c)^j$ and these do not vanish, because $b = 2c$ leads to a point $(c, 2c, c, 2c) \notin \mathcal{X}$. Hence $\phi_4$ is good.

**Case 5:** Suppose $\phi_5 = c + d = 0$. Then $d = -c$. We first compute

$$0 = g(a, b, c, -c) = c^4(1 - a + b)(1 + a - b)(a + b)^2. \tag{34}$$

The first 3 factors are nonzero on $\mathcal{X}$. Hence $b = -a$. When $d = -c$ and $b = -a$ we solve $X_{11}X_{23} - X_{13}X_{21} = 0$ and find that

$$a = c, \quad \text{or} \quad a = \frac{-1}{2c}, \quad \text{or} \quad a = \frac{c}{2c - 1} \quad \text{or} \quad a = \frac{-c}{2c + 1}. \tag{35}$$

Choice 1 gives $(a, -a, a, -a) \notin \mathcal{X}$. Choice 2 gives a point in $\mathcal{Y}$. Choices 3 and 4 respectively lead to $F_1 = 0$ and $F_2 = 0$. Hence $\phi_5$ is good.

**Case 6:** Suppose $\phi_6$ is bad. Setting $\phi_6 = 0$, making the substitution for $b$, then setting $X_G \cdot \nabla \phi_6 = 0$, we get

$$b = \frac{c^2 - cd}{c + d}, \qquad a = \frac{c^2 - cd}{c + d} \quad \text{or} \quad a = \frac{-2c - c^2 d + d^3}{(c + d)^2}.$$

Since $\phi_5$ is good, we can perturb along our $G$-curve to that $c + d \neq 0$ and all our substitutions are well defined. There are 2 choices for $a$. The first choice leads to $G(a, b, c, d) = 0$, so the second choice obtains. The rest of the proof is like Case 1 except now $f/f^*$ and $g/g^*$ have the form $c^i(c + d)^j$ and this expression is good by Case 5. Hence $\phi_6$ is good.

**Cases 7 and 8:** Suppose $\phi_7 = 0$. Solving for $b$ we have

$$b = \frac{c(1 + c + d)}{1 + c - d}. \tag{36}$$

Solving $X_G \cdot \nabla \phi_7 = 0$ for $a$ yields

$$a = \frac{d - cd - d^2}{1 + c - d} \quad \text{or} \quad \frac{d + 5cd + 7c^2d + 3c^3d + 4c^2d^2 - d^3 + cd^3}{-1 - c + c^2 + c^3 - 2d - 6cd - 4c^2d + d^2 + cd^2 + 2d^3}. \tag{37}$$

The first choice leads to $F_2(a, b, c, d) = 0$ and this point does not lie in $\mathcal{X}$. Hence $a$ is the second choice. The rest of the proof is as in Step 1, but

$$\frac{f}{f^*} = \frac{g}{g^*} = \frac{c^2(a + ac - d - ac + cd + d^2)}{(1 + c - d)^4}.$$

The factors $c$ and $(1 + c - d)$ do not vanish in $\mathcal{X}$. The big factor on the right does not vanish because it is also a factor of $F_2(a, b, c, d) \neq 0$. Hence $\phi_7$ is good. $\phi_8$ is good by symmetry.

**Case 9:** Suppose that $\phi_9$ is bad. Solving $\phi(a, b, c, d) = 0$ for $c$ we get a quadratic equation. The two roots $c_1$ and $c_2$ satisfy

$$c_1 + c_2 = \frac{bd^2 + db^2}{bd + 1}, \qquad c_1 c_2 = -1 - bd. \tag{38}$$

The permutation $\pi(a, b, c, d) = (c, d, a, b)$ preserves $\mathcal{D}$. The same arguments as above, with the coordinates permuted, show that $\phi_j \circ \pi$ is good for $j = 1, ..., 8$. Only the badness of $\phi_9 \circ \pi$ can cause $(c, d, a, b) \in \mathcal{D}$. Hence $\phi_9(c, d, a, b) = 0$. Solving $\phi(c, d, a, b) = 0$ for $a$ we get the same result as in Equation 38. In other words, $a, c \in \{c_1, c_2\}$.

The function $\phi_4 \circ \pi = a - c$ is good, so $a$ and $c$ are the *two different solutions* of Equation 38. We set $c = c_1$ and $a = c_2$. Hence $ac + bd + 1 = 0$. This is the first defining relation for $\mathcal{Y}$. As an aside, we have $bd + 1 \neq 0$ because $ac \neq 0$. We also now have

$$a + c = \frac{bd^2 + db^2}{bd + 1} = \frac{bd^2 + db^2}{-ac},$$

which implies that $ac^2 + ca^2 + bd^2 + db^2 = 0$. This is the second defining relation for $\mathcal{Y}$. Hence $(a, b, c, d) \in \mathcal{Y}$, a contradiction. Hence $\phi_9$ is good.

# 4 Cylinders in the Positive Part

## 4.1 Overview

We carry out Step 2 of the outline given §2.9. Recall that $\mathcal{X}_+$ is the subset of $\mathcal{X}$ where all the factors of $F_1$, $F_2$, and $G$ are positive. We also throw out points of the form $(a, b, a, b)$. Let $L_+$ be a level set of $\mathcal{X}_+$ Recall that a $G$-*curve* of $L_+$ is one that is integral to $X_G$. Let $\mathcal{U}$ be the set $(a, b, c, d)$ with $\max(a + b, c + d) = 1$. Here is an outline of what we do in this chapter.

1. In §4.2 we prove the $L_+$ is bounded in $\boldsymbol{R}^4$.

2. In §4.3 we classify the accumulation points of $L_+$ in $\boldsymbol{R}^4 - \mathcal{X}_+$.

3. In §4.4 we combine a monotonicity idea related to Lemma 2.4 with the classification from §4.3 to prove that each $G$-curve intersects $\mathcal{U}$ exactly once. We then use the intersection property to prove that $\mathcal{X}_+$ is path connected.

4. In §4.5 we show that $L_+ \cap \mathcal{U}$ is a finite union of closed loops. We then use a homotopy argument involving the path connectivity of $\mathcal{X}_+$ to show that in fact $L_+ \cap \mathcal{U}$ is just the nice loop from Step 2.

Since $L_+$ is foliated by $G$-curves, each of which intersects $\mathcal{U}$ once, we see that $L_+$ is homeomorphic to the product of an open interval with the loop $L_+ \cap \mathcal{U}$. Hence $L_+$ is a cylinder.

## 4.2 Boundedness of the Level Sets

**Lemma 4.1** *The level set $L_+$ is bounded in $\boldsymbol{R}^4$.*

**Proof:** We work with the functions $g_{ab}$ and $g_{cd}$ from Equation 7.

$$g_{ab} = \frac{1 - a^2 - b^2}{ab}, \qquad g_{cd} = \frac{1 - c^2 - d^2}{cd}.$$

Suppose $\{(a_n, b_n, c_n, d_n)\}$ is an unbounded sequence in $L_+$. It suffices to suppose one of $c_n$ or $d_n$ tends to $\infty$. Since $|c_n - d_n| < 1$, both of these coordinates tend to $\infty$. Hence $g_{cd} \to -2$. We will show that $g_{ab} \to +2$ as $n \to \infty$. This gives $|g_{ab} + g_{cd}| \to 0$ as $n \to \infty$. Since $|g_{ab}^* + g_{cd}^*| \le 2$, we get $G(a_n, b_n, c_n, d_n) \to 0$ on the level set, a contradiction

Passing to a subsequence we can assume that $a_n + b_n > 1$ for all $n$ or

$a_n + b_n < 1$ for all $n$. In the first case $g_{ab} < 2$. Since $g_{ab} + g_{cd} > 0$ and $g_{cd} \to -2$ we must have $g_{ab} \to 2$. Now suppose $a_n + b_n < 1$ for all $n$.

Look at the factor $a - d + ac + bd > 0$ of $F_2$ and note that $c_n < d_n + 1$:

$$0 < a_n - d_n + a_n c_n + b_n d_n < a_n - d_n + a_n(d_n + 1) + b_n d_n =$$

$$2a_n + (a_n + b_n - 1)d_n = (-d_n + b_n d_n) + (a_n d_n + 2a_n). \qquad (39)$$

Since $d_n \to +\infty$, Equation 39 implies that $a_n + b_n \to 1$.

If $a_n, b_n$ remain in a compact subset of $(0, 1)$ we have $g_{ab} \to 2$. We just have to worry about the case that $(a_n, b_n) \to (1, 0)$ or $(0, 1)$. We will consider the second case. The first case has a similar treatment, except that we would re-do Equation 39 with the factor $b - c + ac + bd > 0$ of $F_1$.

Divide the last expression of Equation 39 by $a_n d_n$ and rearrange to get:

$$\frac{1 - b_n}{a_n} < 1 + \epsilon, \qquad \epsilon = \frac{2}{d_n}.$$

Since $d_n \to \infty$ we can take $\epsilon > 0$ as small as we like. But then

$$\frac{1 - a_n^2 - b_n^2}{a_n b_n} < \frac{1 - b_n^2}{a_n b_n} = \frac{1 + b_n}{b_n} \times \frac{1 - b_n}{a_n} < \left(1 + \frac{1}{b_n}\right) \times (1 + \epsilon). \qquad (40)$$

Since $b_n \to 1$, Equation 40 says that $\limsup(g_{ab}) \le 2$. Since $g_{ab} + g_{cd} > 0$ and $g_{cd} \to -2$ we also have $\liminf g_{ab} \ge 2$. Hence $g_{ab} \to 2$. ♠

## 4.3 Classification of the Accumulation Points

**Lemma 4.2** *Up to the permutation $I$ from §5, every accumulation point of $L_+$ not in $\mathcal{X}$ has the following form.*

1. $(0, \bar{b}, \bar{b}, 0)$ *for* $\bar{b} \in [0, 1)$.

2. $(0, 1, 1, 0)$ *or* $(0, 1, 0, 1)$ *or* $(1, 0, 1, 0)$.

3. $(0, 1, \bar{c}, \bar{d})$ *or* $(1, 0, \bar{c}, \bar{d})$ *for* $\bar{c} > 0$ *and* $\bar{d} > 0$ *and* $\bar{c} + \bar{d} > 1$.

**Proof:** Consider a sequence $\{(a_n, b_n, c_n, d_n)\} \in L_+$ converging to some $(\bar{a}, \bar{b}, \bar{c}, \bar{d}) \in \mathbf{R}^4 - L_+$. If $\bar{a}, \bar{b}, \bar{c}, \bar{d} > 0$ then some factor of the numerator of $F_1$ or $F_2$ vanishes at our limit point. But then the function $F_1$ or $F_2$ also vanishes there. This contradicts the fact that $F_1$ and $F_j$ are constant on $L_+$. Hence, at least one of the limit coordinates is 0.

The rest of our proof only uses the fact that $|G|$ is bounded on $L_+$. Since we don't care about the sign of $G$, we can freely use the symmetries $I$ and $J$ from Equation 5 to simplify our work. (Composition with $J$ switches $F_1$ and $F_2$ and negates $G$.) Using $I$ and $J$ we can assume that $\bar{a} = 0$. Since $|a - b| \leq 1$ when all factors of $F_1$ and $F_2$ are positive, we have $\bar{b} \in [0, 1]$.

We use $\sim$ to denote the relation that the ratio of two quantities is asymptotically 1 as $n \to \infty$. We write

$$b_n = 1 - K_n a_n.$$

Let $NF_j$ and $DF_j$ respectively denote the numerator and denominator of $F_j$. We have

$$\lim \frac{DF_j(a_n, b_n, c_n, d_n)}{a_n} = \bar{b}\bar{c}\bar{d}.$$

Let $F_{jkn}$ denote the $k$th factor of $NF_j(a_n, b_n, c_n, d_n)$. The trick in our proof is finding the right factor of $NF_j$ to divide by $a_n$. We find that

$$\frac{F_{11n}}{s_n} \sim 1 + K_n, \quad F_{12n} \to 1 + \bar{c} - \bar{d}, \quad F_{13n} \to 1 - \bar{c} + \bar{d}, \quad F_{14n} \to 2\bar{d}.$$

$$F_{21n} \to 2, \quad F_{22n} \to 1 - \bar{c} + \bar{d}, \quad F_{23n} \to \bar{c} + \bar{d} - 1, \quad \frac{F_{24n}}{a_n} \sim 1 + \bar{c} - K_n\bar{d}. \quad (41)$$

We now distinguish 3 cases:

**Case 1:** Suppose $\bar{b} < 1$. Then $K_n \to +\infty$. Since $a_n^{-1}F_{24n} > 0$ we have $\bar{d} = 0$. Since $c > 0$ and $d > 0$ and $|c - d| < 1$ we have $g_{cd} > -2$. Since $\bar{b} < 1$ and $\bar{a} \to 0$ we have $g_{ab} \to \infty$. Hence $g_{ab} + g_{cd} \to +\infty$ and (given that $|G|$ is bounded) also $g_{ab}^* + g_{cd}^* = a - b + c - d \to 0$. Hence $t = 0$. This gives us $(0, \bar{b}, \bar{b}, 0)$ as the limit.

**Case 2:** Suppose that $\bar{b} = 1$ and $\bar{c}\bar{d} = 0$. Since $|c_n - d_n| < 1$ we have $\bar{c} + \bar{d} \leq 1$. The positivity and asymptotics of $F_{23n}$ gives $\bar{c} + \bar{d} \geq 1$. Hence $\bar{c} + \bar{d} = 1$. The only choices are $(\bar{c}, \bar{d}) = (1, 0)$ or $(0, 1)$.

**Case 3:** Suppose $\bar{b} = 1$ and $\bar{c}\bar{d} > 0$. As in Case 2, the positivity and asymptotics of $F_{23n}$ implies that $\bar{c} + \bar{d} \geq 1$. We will assume that $\bar{c} + \bar{d} = 1$ and derive a contradiction. Since $\bar{c}\bar{d} > 0$ we have $|\bar{c} - \bar{d}| < 1$. But then the last 3 factors in the first row of Equation 41 are positive. This forces $\{K_n\}$ to be bounded. But then $\{a_n^{-1}F_{24n}\}$ is bounded. Since $\bar{c} + \bar{d} - 1 = 0$, we see that $F_{23n} \to 0$. Hence $F_2 \to 0$. But $F_2$ is bounded away from 0 (and indeed constant) on our sequence. This is a contradiction. Hence $\bar{c} + \bar{d} > 1$. ♠

## 4.4  Analysis of Flowlines

Let $\chi$ be a $G$-curve in $L_+$. We orient $\chi$ so that its tangent vectors are positive multiples of $X_G$. As we remarked after Lemma 2.4, both ends of $\chi$ exit every compact subset of $\mathcal{X}_+$. Hence, both ends have at least one accumulation point.

**Lemma 4.3** *The backwards end of any $G$-curve has a unique accumulation point, and it has the form $(x,0,0,x)$ or $(0,x,x,0)$ for some $x \in [0,1)$. The forwards end of any $G$-curve has a unique accumulation point, and it is either $(1,0,1,0)$ or $(1,0,x,y)$ or $(x,y,1,0)$ with $x,y > 0$ and $x + y > 1$.*

**Proof:** Thanks to Equations 19 – 23, the functions $g_{ab}$ and $g_{cd}$ and $g_{ab}^*$ and $g_{cd}^*$ are all monotone along $\chi$. In particular, $a - b$ and $c - d$ are increasing as we move forward along $\chi$.

Suppose that the backwards end of $\chi$ accumulates on $(1,0,x,y)$. But $a - b$ increases along $\chi$ and remains less than 1. This is an immediate contradiction. The same argument, using $c - d$ in place of $a - b$, rules out and $(x,y,1,0)$. Suppose $(0,1,x,y)$ is a backwards accumulation point. Since we have the inequality $a - b + c - d > 0$ in $\mathcal{X}_+$ we must have $x - y \geq 1$. But, again, this contradicts the fact that $c - d$ increases along $\chi$ and always satisfies $c - d < 1$. The same argument rules out $(x,y,0,1)$ as a limit point. Lemma 4.2 now says that any accumulation point has the claimed form.

The uniqueness follows from the characterization of the backwards accumulation points and from the monotonicity of $a - b$ and $c - d$ along $\chi$. One final observation. Given the nature of the backwards limit point, the quantity $a - b + c - d$ converges to 0 at the backwards end of $\chi$.

Suppose that the forward end of $\chi$ accumulates on $(a',0,0,a')$. Then the quantity $a - b + c - d$ converges to 0 in the forward direction along $\chi$. Given the monotonicity of $a - b + c - d$, this is only possible if $a - b + c - d = 0$ along $\chi$, a contradiction. The same argument rules out a forward limit of $(0,b',b',0)$. Another monotonicity argument, as in the backwards case, rules out forward limit points of the form $(0,1,x,y)$ and $(x,y,0,1)$. The only choices left are the ones advertised in the statement of this lemma.

For forward uniqueness, note that $g_{ab}$ and $g_{cd}$ (being monotone increasing and bounded from above by 2) and $g_{ab}^*$ and $g_{cd}^*$ (being monotone decreasing and bounded from below by $-2$) have forward limits along $\chi$. These limits uniquely specify $(1,0,x,y)$ or $(x,y,1,0)$. If *both* $(1,0,x,y)$ and $(x,y,1,0)$ are forward limits, then $\chi$ bounces back and forth repeatedly while exiting every compact subset of $\mathcal{X}_+$, forcing an impossible continuum of limit points. ♠

**Lemma 4.4** *Each G-curve in $L_+$ intersects $\mathcal{U}$ exactly once.*

**Proof:** Let $\chi$ be a $G$-curve. Let us take care of the uniqueness first. When $a, b > 0$, a condition we have on $\chi$, we have $g_{ab} > 2$ if and only if $a + b < 1$. Also, $g_{ab} = 2$ if and only if $a + b = 1$. Since $g_{ab}$ strictly decreases along $\chi$, we have have $g_{ab} = 2$ only once. Likewise we can have $g_{cd} = 2$ only once. Hence we can have $\max(g_{ab}, g_{ac}) = 2$ only once.

Now we turn to the existence of the intersection. The backwards limit point of $\chi$ has the form $(a, b, c, d)$ where $\max(a+b, c+d) < 1$. The forwards limit point has the form $(a, b, c, d)$ where $\max(a + b, c + d) \geq 1$ and we have equality only if the forwards limit point is $(1, 0, 1, 0)$. So, our proof is done unless the forward limit point is $(1, 0, 1, 0)$. We consider this case.

Let $\{a_n, b_n, c_n, d_n\}$ be a sequence along $\chi$ converging to $(1, 0, 1, 0)$. All our proof uses is that the sequences $\{F_n(a_n, b_n, c_n, d_n)\}$ are bounded away from 0. It suffices to show there is some $n$ such that $\max(a_n+b_n, c_n+d_n) > 1$. We assume not and derive a contradiction. We write $a_n = 1 - b_n - h_n$ and $c_n = 1 - d_n - k_n$ with $b_n, d_n, h_n, k_n \geq 0$ and $b_n, d_n, h_n, k_n \to 0$. We have

$$F_1 = \frac{1}{a_n c_n} \times (2 - 2b_n - h_n) \times (2 - 2d_n - k_n) \times$$

$$\frac{2b_n d_n + b_n k_n - (1 - d_n - k_n)h_n}{b_n} \times \frac{2b_n d_n + d_n h_n - (1 + b_n + h_n)k_n}{d_n} <$$

$$3 \times 2 \times 2 \times (2d_n + k_n) \times (2b_n + h_n) \to 0.$$

Hence $F_1 \to 0$ on $L_+$, a contradiction. ♠

**Lemma 4.5** *The space $\mathcal{X}_+$ is path connected.*

**Proof:** By Lemma 4.4, every point of $\mathcal{X}_+$ can be joined to $\mathcal{X}_+ \cap \mathcal{U}$ by a $G$-curve. So, we just have to prove that $\mathcal{X} \cap \mathcal{U}$ is path connected.

Let $\mathcal{U}_{abcd} = \mathcal{U}_{ab} \cap \mathcal{U}_{cd}$. Now we show that we can join any point of $\mathcal{X}_+ \cap \mathcal{U}_{ab}$ to a point of $\mathcal{X}_+ \cap \mathcal{U}_{abcd}$ by a path that remains in $\mathcal{X}_+$. The same argument works with $(c, d)$ replacing $(a, b)$.

Choose $(a, b, c, d) \in \mathcal{X}_+ \cap \mathcal{U}_{ab}$. This point satisfies $a+b = 1$ and $c+d < 1$. We connect our point to a nearby point $(a', b', c', d')$ where $a' - b' \neq c' - d'$. So, without loss of generality assume that $a - b \neq c - d$. Consider the segment $\sigma$ given by $(a, b, c, d) \to (a, b, c+t, d+t)$. We start at $t = 0$ and we end when when we reach $\mathcal{U}_{abcd}$. Along $\sigma$ we have $g_{ab}, g_{cd} \geq 2$ so $g_{ab}+g_{cd} \geq 4$.

The function $g^*_{ab} + g^*_{cd}$ is constant along $\sigma$. Hence the factors of $G$ remain positive along $\sigma$. Consider the factors of $F_1$ and $F_2$. First, $a, b, c, d$ all remain positive along $\sigma$. The factors of the form $1 + \mu - \nu$ are constant along $\sigma$. A typical one is $1 - c + d$. Consider a factor of the form $\zeta = e + \mu - \mu$ with $e = ac + bd$ and $\mu \in \{\pm a, \pm b\}$ and $\nu \in \{\pm c, \pm d\}$. Along $\sigma$ we have $de/dt = 1$ and $d\mu/dt = 0$ and $d\nu/dt = \pm t$. We conclude that $d\zeta/dt \geq 0$. Hence all factors of $F_1$ and $F_2$ remain positive on $\sigma$. Finally, thanks to our initial perturbation, the endpoint of $\sigma$ does not have the form $(a, b, a, b)$.

In $\mathcal{U}_{abcd}$ we have $b = 1 - a$ and $d = 1 - c$. Let $\lambda$ be the line $a = c$. Let $\tau$ be the open triangle $(a, 1 - a, c, 1 - c)$ with $a, c, 1 - a, 1 - c, a + c - 1 > 0$. We have $\mathcal{X}_+ = \mathcal{U}_{abcd} = \tau - \lambda$. The space $\tau - \lambda$ has 2 components. To finish the proof we just have to connect any point in one component to any point in the other using a path in $\mathcal{X}_+$. We start with the point $(3/4, 1/4, 2/3, 1/3) \in \tau - \lambda$ and move linearly to $(3/4, 1/3, 2/3, 1/4)$. Then we move linearly to $(2/3, 1/3, 3/4, 1/4) \in \tau - \lambda$. One can easily check that this bigon remains in $\mathcal{X}_+$. ♠

## 4.5 A Closer Look at the Intersection

**Lemma 4.6** $L_+ \cap \mathcal{U}$ *is compact.*

**Proof:** We will suppose this is false and then derive a contradiction. Let $\{a_n, b_n, c_n, d_n\} \in L_+$ be a sequence of points which exits every compact subset of $\mathcal{U}$. Since $\mathcal{U}$ is defined by a closed condition, our sequence must exit every compact subset of $\mathcal{X}_+$. Without loss of generality assume that $a_n + b_n = 1$ and $c_n + d_n \leq 1$. By Lemma 4.2 there are 4 possible accumulation points: $(0, 1, 0, 1)$ or $(1, 0, 1, 0)$ or $(1, 0, 0, 1)$ or $(0, 1, 1, 0)$. The limit $(0, 1, 0, 1)$ cannot occur because we need $a - b + c - d > 0$. The proof of Lemma 4.4 rules out $(1, 0, 1, 0)$. The symmetry $J$ swaps the remaining cases, and our last arguments never uses $G$. So, it suffices to treat the case of $(0, 1, 1, 0)$.

We set $b_n = 1 - a_n$ and $c_n = 1 - d_n - h_n$. We have $a_n, c_n, h_n \to 0$ and all these are positive. Remembering that $F_1$ is constant on $L_+$, we compute

$$F_1 = \frac{1}{b_n c_n} \times \frac{2a_n}{a_n} \times (2 - 2d_n - h_n) \times (1 - a_n)(2d_n + h_n) \times \frac{2d_n - 2a_n d_n - a_n h_n}{d_n} \leq$$

$$3 \times 2 \times 2 \times (2d_n + h_n) \times 2 \to 0.$$

Hence $F_1 = 0$ on $L_+$, a contradiction. ♠

26

**Lemma 4.7** $L_+$ is transverse to $\mathcal{U}_{ab}$ and to $\mathcal{U}_{cd}$

**Proof:** By symmetry it suffices to consider $\mathcal{U}_{ab}$. Since $L_+$ is smooth it suffices to prove that $X_G$ is not tangent to $\mathcal{U}_{ab}$. The vector $(1, 1, 0, 0)$ is perpendicular to this space, and (setting $b = 1 - a$) we compute

$$X_G \cdot (1, 1, 0, 0) = \frac{4a(1-a)(1+c-d)(1-c+d)}{cd} \neq 0. \qquad (42)$$

This does it. ♠

By transversality and compactness, the intersection $L_+ \cap \mathcal{U}$ is a smooth 1-manifold away from $\mathcal{U}_{abcd}$ and overall a compact topological 1-manifold. A smooth arc which starts in $\mathcal{U}_{ab}$ and hits $\mathcal{U}_{abcd}$ simply continues across the intersection into $\mathcal{U}_{cd}$ as another smooth arc. There is one fine point here. Why couldn't two loops exactly touch along $\mathcal{U}_{abcd}$, making a figure 8? In this case, we could look at the union of $G$-curves through this figure 8 and we would get the product of a figure 8 and an arc. This is not a surface, which contradicts the fact that $L_+$ is a smooth surface. In short $L_+ \cap \mathcal{U}$ is a finite union of $C(L_+)$ closed loops. Recall that such a loop is nice if it intersects $\mathcal{U}_{abcd}$. Let $N(L_+) \leq C(L_+)$ denote the number of nice loops.

**Lemma 4.8** Both $C(L_+)$ and $N(L_+)$ are independent of $L_+$.

**Proof:** Consider $C(\cdot)$ first. Imagine that we have a closed arc in $\mathcal{X}_+$. We think of $C(\cdot)$ as a function on this arc. Since every single intersection $L_+ \cap \mathcal{U}$ is a closed topological 1-manifold, the various loops cannot merge or split into two as we go along the arc. Also, by compactness, none of the loops can exit all compact subsets of $\mathcal{U}$. Finally, no loop can shrink to a point. We conclude that $C(\cdot)$ is constant along our arc. Since $\mathcal{X}_+$ is path connected, we see that $C(\cdot)$ is globally constant. The argument for $N(\cdot)$ is the same. ♠

**Lemma 4.9** $N(L_+) = 1$.

**Proof:** Set $x^* = 1 - x$. At the point $(a, a^*, c, c^*)$ we have $F_1 = 16a^*c^*$ and $F_2 = 16ac$. There are at most 2 values of $(a, c)$ which gives any particular choice $(F_1, F_2)$. The number of these solutions is twice $N(L_+)$ because each nice loop hits $\mathcal{U}_{abcd}$ twice. We conclude that $N(L_+) \leq 1$. At the same time, we have $N(L_+) \geq 1$ because some level sets obviously intersect $\mathcal{U}_{abcd}$. The two bounds give $N(L_+) = 1$. ♠

**Lemma 4.10** $C(L_+) = 1$.

**Proof:** The space $\mathcal{X}_+ \cap \mathcal{U}$ is foliated by its intersection with the level sets, and each intersection is a finite number of loops. Call a point in $\mathcal{X}_+ \cap \mathcal{U}$ *happy* if it lies on a nice loop and otherwise *unhappy*. It suffices to prove that all points are happy.

By compactness of the intersections, and continuity of the intersections, the set of happy points is closed. We claim that the set of unhappy points is also closed. Assuming this claim, and the fact that $\mathcal{U} \cap \mathcal{X}_+$ is path connected, we see that either all points are happy or all points are unhappy. Since some points are happy, all points are happy.

If our claim is false then we can find a sequence $\{\gamma_n\}$ of loops which avoid $\mathcal{U}_{abcd}$, which remain in a compact subset of $\mathcal{U} \cap \mathcal{X}_+$, and which touch $\mathcal{U}_{abcd}$ in the limit. Each of our loops lies in one of $\mathcal{U}_{ab}$ or $\mathcal{U}_{cd}$. This means that the limit loop $\gamma$ only touches $\mathcal{U}_{abcd}$ in a single poiint. But then $\gamma \cap I(\gamma)$ are a pair of loops making a figure 8. This is something we have already discussed and ruled out. This proves the claim. ♠

Now we know that $L_+ \cap \mathcal{U}$ is a single nice loop. Hence $L_+$ is an open cylinder. This completes our proof. We also mention, as a byproduct of our proof, that every level set of $\mathcal{X}_+$ contains exactly 2 points of the form $(a, a^*, c, c^*)$. From this we see that $F_1, F_2, G \in (0, 16)$ on $\mathcal{X}_+$. I discovered this last fact numerically but could't find a purely algebraic proof.

# 5 Intrinsic Boundedness and Concavity

## 5.1 Overview

We carry out Step 3 of the outline in §2.9. We show that each level set $L_+$ of $\mathcal{X}_+$ is intrinsically bounded and has boundaries which are locally concave everywhere except 2 points. Let $\Delta$ be as in Equation 4. Let $\iota_5 = A\delta A\delta A$. Both these maps are isometric involutions with respect to any flat metric on $L_+$ coming from the integrable structure.

Let $L'_+$ denote the subset of $L_+$ consisting of points $(a, b, c, d)$ with $\max(a+b, c+d) < 1$. Note that $L'_+$ is foliated by $G$-arcs which connect the back end of $L_+$ to the nice loop. In particular, $L'_+$ is a sub-cylinder of $L_+$. In §5.2 we prove two results:

1. $\Delta(L_+) = L_+$ and $\Delta$ swaps the ends of $L_+$.

2. $\iota_5(L'_+) = L'_+$ and $\iota_5$ swaps the ends of $L'_+$.

What makes this powerful is that the front end of $L'_+$ lies in $\mathcal{X}_+$, and we can make direct calculations on it. Using the intrinsic isometry $\iota_5$ we can transfer metric information about the front end of $L'_+$ to the back end of $L_+$. Using $\Delta$ we can then transfer metric information about the back end of $L_+$ to metric information about the front end of $L_+$. To put this another way, suitable compositions of $\Delta$ and $\iota_5$ blow up the ends of $L_+$ so that we can see them. We will use this technique in §5.4 to prove the intrinsic boundedness result and in §5.5 to prove the concavity result.

## 5.2 First Reversal Lemmas

**Lemma 5.1 (Reversal I)** $\Delta(L_+) = L_+$ and $\Delta$ swaps the ends of $L_+$.

**Proof:** We already know that $\mathcal{X}_+$ is path connected. A single evalution, say for the point $(1/4)(2, 1, 2, 1)$, suffices to show that $\Delta(\mathcal{X}_+) \cap \mathcal{X}_+ \neq \emptyset$. Since the component functions of $\Delta$ are positive and since $F_j \circ \Delta = F_j$ and $G \circ \Delta = G$ we see that $\Delta$ cannot map any point of $\mathcal{X}_+$ into the boundary of $\mathcal{X}_+$. This would cause some invariant to vanish. Since $\mathcal{X}_+$ is connected, this implies that $\Delta(\mathcal{X}_+) \subset \mathcal{X}_+$. Since $\Delta$ is an involution we have $\Delta(\mathcal{X}_+) = \mathcal{X}_+$. Since $\Delta$ preserves both invariants we must have $\Delta(L_+) = L_+$. Since $\Delta$ preserves both invariants and negates the symplectic form, we see that $\Delta$ is an isometry of $L_+$ which reverses the direction of the $G$-curves. Hence $\Delta$ swaps the ends of $L_+$. ♠

## 5.3 Second Reversal Lemma

Let $L'_+$ denote the subset of $L_+$ consisting of arcs of $G$-curves which join points on the nice loop $L_+ \cap \mathcal{U}$ to the backwards end of $L_+$. This definition makes sense because each $G$-curve intersects the nice loop once.

**Lemma 5.2 (Reversal II)** $\iota_5(L'_+) = L'_+$ and $\iota_5$ swaps the ends of $L'_+$.

The rest of this section is devoted to proving this result.

**Lemma 5.3** For any $p \in L_+ \cap \mathcal{U}$ we have $\iota_5(p) = (0, x, x, 0)$ or $(x, 0, 0, x)$.

**Proof:** Recall that $\mathcal{U}_{ab}$ consists of points $(a, b, c, d)$ with $a + b = 1$ and $c + d \leq 1$. For $(a, 1 - a, c, d) \in L_+$ we compute

$$\iota_5(a, 1 - a, c, d) = (0, x, x, 0), \qquad \beta = \frac{1 - (c + d)}{(c + d) - (c - d)^2}. \qquad (43)$$

A similar calculation works for points in $\mathcal{U}_{cd}$ and there we get $(x, 0, 0, x)$. ♠

**Lemma 5.4** The map $\iota_5$ is well-defined and real analytic in the cube $(0, 1)^4$. If $(a', b', c', d') = \iota_5(a, b, c, d)$ and $(a, b, c, d) \in L'_+$ then $(a', d') \neq (0, 0)$ and $(b', c') \neq (0, 0)$.

**Proof:** Let $x^* = 1 - x$. The denominator of each coordinate equals one of two products:

$$(b + c - ac - bd)\mu, \qquad (a + d - ac - bd)\mu,$$

$$\mu = aca^*c^* + bdb^*d^* + abcc^* + abdd^* + cdaa^* + cdbb^* + 2abcd.$$

These do not vanish on $(0, 1)^4$ and so $\iota_5$ is well-defined and real analytic.

When we solve $a' = d' = 0$ we find that either $cd = 0$ or $a + b = 1$ or

$$a = \frac{d(1 + c - d)}{1 - (c + d)}, \qquad b = \frac{c(1 - c + d)}{1 - (c + d)}. \qquad (44)$$

The first case gives points not in $\mathcal{X}_+$. The second case gives points not in $L'_+$. In the third case, Equation 44 leads to $a - b + c - d = 0$, so that $(a, b, c, d) \notin \mathcal{X}_+$. Hence $(a, d') \neq (0, 0)$. The same argument works for $(b', c')$ and this also follows from symmetry. ♠

Let $\mathcal{X}'_+$ denote the subset of $\mathcal{X}'_+$ consisting of those points $(a, b, c, d)$ with $a + b < 1$ and $c + d < 1$. Call a point $p \in \mathcal{X}'_+$ *good* if $\iota_5(p) \in \mathcal{X}'_+$. The set of good points is non-empty. For instance, $p = (1/2, 2/3, 2/3, 1/4)$ is good. By Lemma 5.4, the set of good points is open.

**Lemma 5.5** *The set of good points is closed.*

**Proof:** Let $p = \lim p_n$ be the limit of a sequence of good points. By Lemma 5.4, the point $q = \iota_5(p)$ is well-defined, and the limit of a sequence of points $\{q_n\}$ where $q_n = \iota_5(p_n)$. We suppose $p$ is not good and we derive a contradiction. We know that $q \notin \mathcal{X}'_+$. If $q \in \mathcal{X}_+$ then we must have $q \in \mathcal{U}$. But then, since $\iota_5$ is an involution, Lemma 5.4 implies that $p = \iota_5(q)$. But this contradicts Lemma 5.3. Hence $q \in \mathbf{R}^4 - \mathcal{X}_+$.

In our proof of Lemma 4.3 we did not really use the fact that we were taking accumulation points of a single level set. The proof there just requires that the sequences $\{F_j(a_n, b_n, c_n, d_n)\}$ are bounded away from 0. Hence $q$ has the form given in the conclusion of Lemma 4.3. Lemma 5.4 rules out $q = (0, x, x, 0)$ or $q = (x, 0, 0, x)$. Since $q$ is the limit of points with $\max(a_n + b_n, c_n + d_n) < 1$ we cannot have $q = (1, 0, x, y)$ etc. with $x + y > 1$. The only cases are $q = (1, 0, 1, 0)$ or $q = (0, 1, 0, 1)$. Since $G(q_n) > 0$ we cannot have $q = (0, 1, 0, 1)$. If $q = (1, 0, 1, 0)$ then having $q_n \to q$ violates the proof of Lemma 4.4 because $\{F_j(q_n)\}$ is bounded away from 0 for $j = 1, 2$. ♠

The same proof that $\mathcal{X}_+$ is path connected shows that $\mathcal{X}'_+$ is path connected. Since the subset of good points is non-empty, open, and closed, all points are good. Hence $\iota_5(\mathcal{X}'_+) \subset \mathcal{X}'_+$. Since $\iota_5$ is an involution, we have $\iota_5(\mathcal{X}'_+) = \mathcal{X}'_+$. Since $F_j \circ \iota_5 = F_j$ we see that $\iota_5(L'_+) = L'_+$ for all level sets $L_+$ of $\mathcal{X}_+$. Finally $\iota_5$ negates the symplectic form and preserves the invariants. Hence $\iota_5$ reverses the direction of the $G$-curves in $L'_+$. Hence $\iota_5$ swaps the ends of $L'_+$. This completes the proof of the Reversal Lemma II.

## 5.4 Intrinsic Boundedness

We choose a flat metric on $L_+$ coming from the integrable structure. The result is independent of choice. By compactness, every point of $p \in L_+$ is (intrinsically) less than $D_p$ units from every point of $L_+ \cap \mathcal{U}$ for some constant $D_p$ which depends on $p$. But now we apply $\iota_5$ and conclude that the same boundedness result holds for the backwards end of $L_+$. Next, we apply $\Delta$ and conclude that the same boundedness result holds for the forwards end of $L_+$. Putting these results together we see that $L_+$ is intrinsically bounded.

## 5.5 Local Convexity

Now we show that $L_+$ is locally concave near $\partial L_+$ except for 2 points on each boundary component. Given the properties of $\iota_5$ and $\Delta$, and symmetry, it

suffices to prove that $L'_+$ is locally concave along the nice loop at all points of $\mathcal{U}_{ab} - \mathcal{U}_{cd}$. Recall that $X_j = X_{F_j}$ is the Hamiltonian vector field associated to our invariant $F_j$. Let

$$Y = \alpha_1 X_1 + \alpha_2 X_2, \qquad \alpha_1 = 1 + c - d, \qquad \alpha_2 = 1 - c + d, \qquad (45)$$

Let $\phi(a, b, c, d) = a + b - 1$ be the defining function for $\mathcal{U}_{ab}$. We already know that $Y$ is tangent to $L_+$. We compute that $Y \cdot \nabla \phi = 0$ when $\phi = 0$, which shows that $Y$ is also tangent to $\mathcal{U}_{ab}$. Hence $Y$ is tangent to the nice loop $\lambda$ at points of $\mathcal{U}_{ab}$.

The Hessian of the defining function is the matrix $Q$ given by

$$Q_{ij} = \partial_{X_i} \partial_{X_j} \phi = X_i \cdot \nabla(X_i \cdot \nabla \phi). \qquad (46)$$

**Lemma 5.6** *The local convexity in the intrinsic metric is equivalent to the statement that*

$$q = Q(\alpha_1, \alpha_2) = \sum_{i=1}^{2} \sum_{j=1}^{2} Q_{ij} \alpha_i \alpha_j \neq 0 \qquad (47)$$

*at points along the nice loop.*

**Proof:** Let $E : L_+ \to \mathbf{R}^2$ be the coordinate system giving the flat structure on $L_+$. By construction $E_*(X_j) = e_j$, the $j$th coordinate vector field. The defining function for $E(\lambda)$ is given by $f = \phi \circ E^{-1} = 0$. The vector field $E_*(Y) = (\alpha_1, \alpha_2)$ is tangent to $E(\lambda)$. The curve $f$ is locally convex $E(\lambda)$ at the point of interest if $Q(\alpha_1, \alpha_2) \neq 0$, where $Q_{ij} = \partial_i \partial_j f$ is the usual Hessian in the plane. But $Q_{ij}$ agrees with the version given in Equation 46, by naturality. Thus, to test local convexity in the intrinsic metric, we just need to check that $q$ in Equation 47 is nonzero. ♠

We compute that

$$q = \frac{8a(1-a)(1 + c - d)^2(1 - c + d)^2(c + d - 1)(c + d - (c - d)^2)}{c^2 d^2} < 0.$$

At points of $\mathcal{U}_{ab} - \mathcal{U}_{cd}$ we have $c + d - 1 < 0$ and all other terms are positive. Since $c, d \in (0, 1)$ we have $|c - d| < c + d$. So, the last factor in the numerator is positive. A single plot is enough to show that the negative sign determines concavity rather than convexity with respect to the side of the arc lying in $L'_+$.

32

# 6 The Generic Convex Case

## 6.1 The Action in the Cylinder

We carry out Steps 4 and 5 of the outline given in §2.9. Recall that $L_+ \subset \mathcal{X}_+$ is one of our cylinder level sets. Let $C_+ = L \cap \mathcal{C}$. All points $(a, b, c, d) \in C_+$ satisfy $\min(a + b, c + d) > 1$. Hence $C_+$ is disjoint from the nice loop $\lambda \subset L_+$ and therefore lies to one side of it.

**Lemma 6.1** $C_+$ *is the subset of* $L_+$ *consisting of points* $(a, b, c, d)$ *with* $\max(a + c, b + d) > 1$.

**Proof:** All points $(a, b, c, d) \in C_+$ satisfy $\min(a + b, c + d) > 1$. Conversely, the conditions $a + b > 1$ and $c + d > 1$ and $|a - b| < 1$ and $|c - d| < 1$ together imply that such a point represents a convex 8-gon. ♠

Let $\widetilde{L}_+$ be the universal cover of $L_+$, given the intrinsic metric. The map $I$ is an isometry of $L_+$ which preserves the ends, preserves $\lambda$, swaps the cusps of $L_+$ and also swaps the cusps of $\lambda$. From all this information, we conclude that $I$ lifts to a translation of $\boldsymbol{R}^2$ which preserves $\widetilde{L}_+$ and $\widetilde{C}_+$ and $\widetilde{\lambda}$ and moves the cusps 1 click, so to speak. Figure 5, a hand-drawn cartoon, shows what we mean.


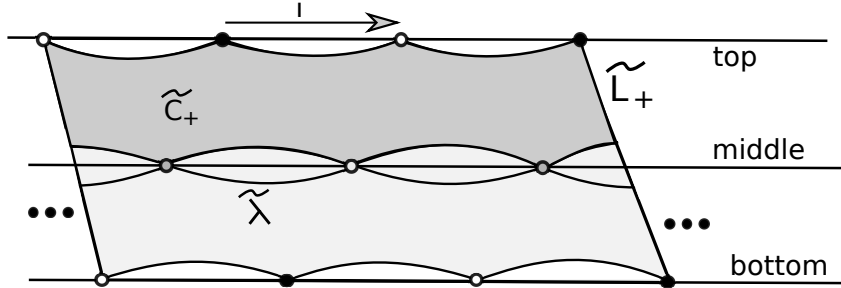
Figure 5: The action of $I$ on the universal cover

Given the action of $I$, the lifts of the cusps of either end of $L_+$ lie on straight lines. Likewise the lifts of the cusps of $\lambda$ lie on a straight line. We called these lines the top, bottom, and middle in our outline.

**Lemma 6.2** *The middle line lies strictly between the top and bottom lines.*

**Proof:** We rotate so that our lines are horizontal and the top line is on top, as in Figure 5.

Let $L'_+$ be the cylinder considered in the previous chapter. Because the ends of $L'_+$ are concave except at the cusps, $\widetilde{L}'_+$ lies between the middle and bottom lines, and only accumulates on these lines at the cusps. Hence the middle line lies above the bottom line.

Suppose that the middle and top line coincide. Then the cusps of $\widetilde{\lambda}$ must lie on the top line. But the $G$-curves through the cusps of $\lambda$ continue for some time before exiting $L_+$. In $\mathbf{R}^2$ the corresponding straight line segments travel upwards before exiting $\widetilde{L}_+$. Since $\widetilde{L}_+$ lies below the top line, this means that the cusps of $\widetilde{\lambda}$ lie below the top line. ♠

The element $\iota_3$, like $\Delta$ and $\iota_5$ which we considered in the previous chapter, is a involution which reverses the directions of the $G$-curves. This means that $\iota_3$ lifts to give an order 2 rotation of $\mathbf{R}^2$ which preserves $\widetilde{C}_+$. Given our description of $\widetilde{C}_+$ (notably the fact that $\widetilde{C}_+$ accumulates on the cusps of $\widetilde{\lambda}$) we see that the lift of $\iota_3$ swaps the top and middle lines. Likewise, the lift of $\Delta$ is a rotation which swaps the top and bottom lines.

This description justifies Equation 27.

## 6.2   Getting to the Positive Part

Our proof of Theorem 1.1 is almost done in the generic convex case. We just have to justify our claim that we can always take a potential counter example to lie in $\mathcal{X}_+$.

Recall from Lemma 2.2 that $\mathcal{C} - \mathcal{I} - \mathcal{I}^*$ has 4 components depending on the signs of $g_{ab} + g_{cd}$ and $g^*_{ab} + g^*_{cd}$. We denote these components by $\mathcal{C}_{++}$, etc. The first sign indicates the sign of $g_{ab} + g_{cd}$. The maps $\sqrt{I}$ and $J$ preserve each of $\mathcal{C}, \mathcal{I}, \mathcal{J}$. Thus each of these maps permutes our 4 components. Making a single evaluation is enough to verify the following action:

$$\sqrt{I}: \qquad \mathcal{C}_{++} \leftrightarrow \mathcal{C}_{--}, \qquad \mathcal{C}_{+-} \leftrightarrow \mathcal{C}_{-+}.$$

$$\sqrt{J}: \qquad \mathcal{C}_{++} \leftrightarrow \mathcal{C}_{+-}, \qquad \mathcal{C}_{-+} \leftrightarrow \mathcal{C}_{--}.$$

Given any $p \in \mathcal{C} - \mathcal{I} - \mathcal{J}$ there is some word $\gamma$ in $I$ and $\sqrt{J}$ such that $\gamma(p) \in \mathcal{C}_{++} \subset \mathcal{X}_+$. If $p$ is a counterexample to Theorem 1.1, then so is $\gamma(p)$, because $\gamma(p)$ is affinely equivalent to $p$ up to dihedrally relabeing.

This completes the proof of Theorem 1.1 in the generic case. The work in [21] takes care of the 8-gons with 4-fold rotational symmetry, and in the next chapter we will deal with the inscribed and circumscribed cases.

# 7 The Inscribed and Circumscribed Cases

We carry out Step 6 of our outline in §2.9 and thereby finish the proof of Theorem 1.2. We also prove Theorem 1.3. Let $\mathcal{CI}$ and $\mathcal{CI}^*$ respectively be the set of inscribed and circumscribed convex points.

**Lemma 7.1** $\mathcal{CI}^*$ *is forward $T_3$-invariant and $\mathcal{CI}$ is backwards $T_3$-invariant.*

**Proof:** We prove the first statement. The second statement follows from the first statement and duality. The defining equation for $\mathcal{I}^*$ is $a - b + c - d = 0$. A calculation shows that this is $T_3$ invariant. Hence $\mathcal{I}^*$ is $T_3$-invariant. (Again, this is a special case of a result in [2].) Let $P_1, ..., P_8$ be the points of $\xi$. Let $\sigma_j = \overline{P_j P_{j+3}}$. Suppose that the lines extending $\sigma_1, \sigma_2, \sigma_3$ intersect at a single point. Then the points $P_1, ..., P_6$ are the vertices of a circumscribed hexagon, by the converse of Brianchon's Theorem. This is impossible for a circumscribed 8-gon: $P_1 P_6$ is not tangent to the supposedly inscribed ellipse. Figure 7 illustrates this.
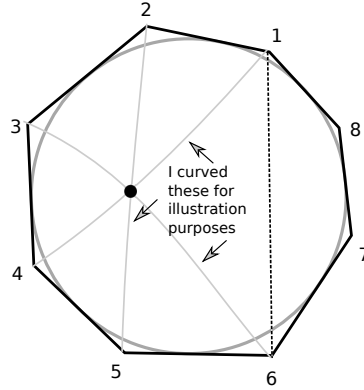


Figure 7: An impossible situation for a circumscribed octagon

Now we know that the lines extending $\sigma_1, \sigma_2, \sigma_3$ do not intersect at a single point. By symmetry the same goes for all $\sigma_i$. Hence, as we vary $P \in \mathcal{CI}^*$ the image $T_3(P)$ is never degenerate. When $P$ is regular, $T_3(P)$ is convex. So, by continuity this holds for all $P \in \mathcal{CI}^*$. Also, $T_3(\xi)$ is again circumscribed because $\mathcal{I}^*$ is $T_3$-invariant. ♠

Let $\Pi_k$ denote the plane consisting of points $(x + k, x - k, y - k, y + k)$. The space $\mathcal{I}^*$ is partitioned into these planes. Let

$$h = -g_{ab} \circ (A\Delta)|_{\Pi_k} = \frac{4k^3 - x + y - 4kxy}{(k - x)(k + y)}. \tag{48}$$

35

Let $L(k, \ell) \subset \Pi_k$ be the level set $h^{-1}(\ell)$.

**Lemma 7.2** $T_3^4$ preserves $L(k, \ell)$ and the action is conjugate to a linear fractional transformation acting on the Riemann sphere.

**Proof:** Calculations show that $T_3^2(\Pi_k) = \Pi_{-k}$ and, when $p \in \Pi_k$,

$$\psi \circ T_3(p) = -i\psi(p), \qquad \psi(a, b, c, d) = h(a, b, c, d) + ih(b, a, d, c). \qquad (49)$$

Hence $T_3^4(L(k, \ell)) = L(k, \ell)$. Solving $h(x, y) = \ell$ and clearing denominators, we get the quadratic equation

$$(\ell - 4k)xy + (1 + k\ell)x - (1 + k\ell)y - (4k^3 - k^2\ell). \qquad (50)$$

This defines a projective curve in $\boldsymbol{CP}^2$ biholomorphic to the Riemann sphere. Under this identification, the automorphism $T_3^4$ is a linear fractional transformation. ♠

Let $\phi_{k,\ell}$ be the linear fractional transformation conjugate to the action extending $T_3^4$ on $L(k, \ell)$. Note that $L(k, \ell)$ contains convex points iff $|k| < 1/2$ and $|\ell| < 2$. Let $\mathcal{K}$ denote this set of $(k, \ell)$.

**Lemma 7.3** If $(k, l) \in \mathcal{K}$ then $\phi_{k,\ell}$ is a hyperbolic linear transformation. The attracting fixed point is convex Poncelet and the repelling fixed point is (up to rotation) the star-reordering of the attracting fixed point.

**Proof:** In $L(k, \ell)$ we can directly solve the equation $\phi_{k,l}(z) = z$ for $x$ and $y$. There are (formally) two solutions $(x_0, -y_0)$ and $(y_0, -x_0)$, where

$$x_0 + y_0 = \frac{2(4k - \ell)(k\ell - 1)}{(2 + \ell)(2 - \ell)}, \qquad x_0 y_0 = \frac{-2 - 4k + 4k\ell - k^2\ell^2}{(2 + \ell)(2 - \ell)}. \qquad (51)$$

The polynomial $t^2 - (x_0 + y_0)t + x_0 y_0$ has discriminant

$$D = 4(1 + 4k^2 - 2k\ell)((8 - \ell^2) - 8k\ell + 4(k\ell)^2). \qquad (52)$$

We have $D > 0$ when $(k, \ell) \in \mathcal{K}$. Thus we get 2 distinct real solutions. A calculation shows that $g_{ab} + g_{cd} = 0$ for the solutions. Since $g_{ab}^* + g_{cd}^* = 0$ as well, any non-degenerate fixed point is Poncelet.

The map $\phi_{k,\ell}$ has 2 real fixed points and preserves the circle in $\boldsymbol{C} \cup \infty$ corresponding to the real points. Hence $\phi_{k,\ell}$ is either hyperbolic or elliptic of

order 2. Since $\mathcal{K}$ is connected the trivial elliptic option cannot occur. Hence $\phi_{k,\ell}$ is hyperbolic.

The fixed points have the form $(a, b, c, d)$ and $-(c, d, a, b)$. Up to rotation, the corresponding polygons are star-reorderings of each other. Given the forward invariance of $\mathcal{CI}^*$, one of the fixed points $(a, b, c, d)$ is the limit of convex 8-gons in $L(k, \ell)$ This gives us

$$|a - b| = |k| < 1, \qquad |c - d| = k < 1, \qquad a + b \geq 1, \qquad c + d \geq 1.$$

If $a + b = 1$ then $g_{ab}(a, b, c, d) = 2$. But then $g_{cd}(a, b, c, d) = -2$. This is not possible for a finite pair $(c, d)$. Hence $a + b > 1$. Likewise $c + d > 1$. Hence $(a, b, c, d)$ gives a nontrivial convex 8-gon. From the calculation above, this 8-gon is Poncelet. The other fixed point is thus star-convex Poncelet. Given the forward invariance of $\mathcal{CI}^*$, the convex fixed point must be attracting. ♠

Thus, the backwards $T_3^{4n}$ iterates of any point of $\mathcal{CI}^* - \mathcal{CI}$ either accumulate on a star-convex 8-gon or become undefined. In either case, the backwards $T_3$-orbit of any point of $\mathcal{CI}^* - \mathcal{CI}$ eventually exits $\mathcal{CI}^*$. Dually, the forwards $T_3$-orbit of any point of $\mathcal{CI} - \mathcal{CI}^*$ eventually exits $\mathcal{CI}$. This completes Step 6 of the outline in §2.9. Our proof of Theorem 1.2 is done.

If we forget about the labelings, we can say more. Since $T_3$ fixes Poncelet polygons up to relabelings, we see that actually $T_3^n(\xi)$ converges to a convex Poncelet 8-gon as $n \to +\infty$. That is, we don't have to restrict our iterates to multiplies of 4 to get the convergence. This (and duality) finishes the proof of Theorem 1.3 .

# References

[1] A. I. Bobenko, T. Hoffmann, Yu. B. Suris, *Hexagonal circle patterns and integrable systems: patterns with the multi-ratio property and Lax equations on the regular triangular lattice*, arXiv:0104244 (2001)

[2] L. S. Evans and J. F. Rigby *Octagrammum Miysticum and the Golden Cross Ratio*, The Mathematical Gazette, Vol 86, No 505 (Mar. 2002) pp 35-43

[3] M. Glick, *The Limit Point of the Pentagram Map*, International Mathematics Research Notices 9 (2020) pp. 2818–2831

[4] M. Glick, *The pentagram map and $Y$-patterns*, Adv. Math. **227**, 2012, pp. 1019–1045.

[5] M. Gekhtman, M. Shapiro, S.Tabachnikov, A. Vainshtein, *Higher pentagram maps, weighted directed networks, and cluster dynamics*, Electron. Res. Announc. Math. Sci. **19** (2012), pp. 1–17

[6] L. Halbeisen and N. Hungerbuhler, *A Simple proof of Poncelet's Theorem (on the occasion of its bicentennial)* Amer. Math. Monthly, **122** No. 6, (2015) pp 537-551

[7] A. Izosimov, *The pentagram map, Poncelet polygons, and commuting difference operators*, arXiv 1906.10749 (2019)

[8] B. Khesin, F. Soloviev *Integrability of higher pentagram maps*, Mathem. Annalen. Vol. 357 no. 3 (2013) pp. 1005–1047

[9] B. Khesin, F. Soloviev *The geometry of dented pentagram maps*, J. European Math. Soc. Vol 18 (2016) pp. 147 – 179

[10] Wolfram Research Inc., *Mathematica*, Wolfram Programming Lab, Champaign, IL (2021)

[11] G. Mari Beffa, *On Generalizations of the Pentagram Map: Discretizations of AGD Flows*, Journal of Nonlinear Science, Vol 23, Issue 2 (2013) pp. 304–334

[12] G. Mari Beffa, *On integrable generalizations of the pentagram map* Int. Math. Res. Notices (2015) (12) pp. 3669-3693

[13] Th. Motzkin, *The pentagon in the projective plane, with a comment on Napier's rule*, Bull. Amer. Math. Soc. **52**, 1945, pp. 985–989.

[14] V. Ovsienko, R. E. Schwartz, S. Tabachnikov, *The pentagram map: A discrete integrable system*, Comm. Math. Phys. **299**, 2010, pp. 409–446.

[15] V. Ovsienko, R. E. Schwartz, S. Tabachnikov, *Liouville-Arnold integrability of the pentagram map on closed polygons*, Duke Math. J. Vol 162 No. 12 (2012) pp. 2149–2196

[16] B. Rodin and D. Sullivan, *The Convergence of Circle packings to the Riemann Mapping Theorem*, J. Diff. Geom. **26** (1987) pp. 349–360

[17] O. Schramm, *Rigidity of Infinite (circle) Packings*, J.A.M.S., Vol 4, No. 1, (1991) pp 127–149

[18] R.E. Schwartz, *The pentagram map*, Exper. Math. **1**, 1992, pp. 71–81.

[19] R. E. Schwartz, *Discrete monodromy, pentagrams, and the method of condensation*, J. of Fixed Point Theory and Appl. **3**, 2008, pp. 379–409.

[20] R. E. Schwartz, *The Poncelet Grid*, Advances in Geometry Vol. 7 (2006) pp. 157-175

[21] R. E. Schwartz, *Survey Lecture on Billiards*, Proceedings of the 2002 International Congress of Mathematicians, I.M.U. Press (2021)

[22] R. E. Schwartz, *A Textbook Case of Pentagram Rigidity*, arXiv 2108-07604 preprint (2021)

[23] R. Schwartz, S. Tabachnikov, *Elementary surprises in projective geometry*, Math. Intelligencer Vol. 32 (2010) pp 31–34.

[24] J. Silverman, *The arithmetic of dynamical systems*, Graduate Texts in Mathemtics **241** (2007) Springer

[25] F. Soloviev *Integrability of the Pentagram Map*, Duke Math J. Vol 162. No. 15, (2012) pp. 2815 – 2853

[26] M. Weinreich, *The Algebraic Dynamics of the Pentagram Map*, (2021) arXiv: 2104.06211